A wave of hematopoietic stem cell-derived T/ILC-restricted progenitors initiates thymopoiesis and shapes the embryonic thymus architecture.

Ramy ELSAID[1-3], Sylvain Meunier[1-3], Odile Burlen-Defranoux[1-3], Francisca Soares-da-Silva[1,2,6], Thibaut Perchet[1-3], Lorea Iturri[4,5], Laina Freyer[4], Paulo Vieira[1-3], Pablo Pereira[1-3], Rachel Golub[1-3], Antonio Bandeira [1-3], Elisa Gomez Perdiguero[4] & Ana Cumano[1-3]

[1]Unit of Lymphopoiesis, Immunology Department, Institut Pasteur, Paris, France. [2]INSERM U1223, Paris, France. [3]Université Paris Diderot, Sorbonne Paris Cité, Paris, France.
[4]Macrophages and Endothelial cells group, Development and Stem Cell Biology Department, Institut Pasteur, Paris, France. [5]Cellule Pasteur UPMC, University Pierre et Marie Curie.
[6]i3S – Instituto de Investigação e Inovação em Saúde, Universidade do Porto, 4200-135, Porto, Portugal.
Correspondence should be addressed to A.C. (ana.cumano@pasteur.fr).

SUMMARY

Multiple waves of hematopoietic progenitors with distinct lineage potentials are differentially regulated in time and space. The site of origin and the cellular outputs of the first wave of thymic seeding progenitors remain unclear. Here we show that these progenitors are T/ILC restricted and unique in generating lymphoid tissue inducer cells, in addition to embryonic-derived invariant $V\gamma5^+$ $\gamma\delta$T cells that are both essential for the development of thymic medullary cells and thus shape the thymic architecture. We further show that all lymphoid progenitors are exclusively of hematopoietic stem cell origin, despite the temporal overlap between thymopoiesis initiation and the transient expression of lymphoid transcripts in yolk sac precursors. This early transient expression does not alter their strict erythro-myeloid differentiation potential. Our work highlights the relevance of the developmental timing on the emergence of different lymphoid subsets required for the establishment of a functionally diverse immune system.

INTRODUCTION

Three lymphoid subsets develop exclusively during embryonic life, they comprise T lymphocytes expressing Vγ5 that reside in the skin, also named dendritic epidermal-like T cells (DETC), Vγ6 that reside in the lungs and in the genital urinary tract and lymphoid tissue inducers (LTis), a subset of group 3 innate lymphoid cells (ILC3). Both $V\gamma5^+$ T cells and LTis are required for the development of medullary thymic epithelial cells (mTECs), through TNFRSF signaling, a mechanism which is only conserved in prenatal stages (Alves et al., 2014; Boyden et al., 2008; Roberts et al., 2012; Rossi et al., 2007). LTis are also required for secondary lymphoid tissue organization (Cupedo and Mebius, 2003; Cupedo et al., 2002) whereas Vγ6 contributes to remodeling of the tissues they colonize (Papotto et al., 2017).

During embryogenesis, the thymus is colonized by two waves of hematopoietic progenitors named thymic seeding progenitors (TSP), with distinct potentials (Cumano et al., 2019; Ramond et al., 2013). The first wave of TSP follow a unique developmental program as they share phenotype, transcriptional signature and restricted T cell differentiation potential with HSA^{lo} $\alpha4\beta7^-$ fetal liver (FL) common lymphoid progenitors (CLPs) (Berthault et al., 2017; Ramond et al., 2013). These CLPs are no longer found after E15.5, a stage after which the thymus is colonized by a second wave of TSPs that share phenotype, transcriptional signature and differentiation potential with lympho-myeloid primed progenitors (LMPPs) (Berthault et al., 2017; Bhandoola et al., 2007; Luc et al., 2012; Ramond et al., 2013). Because the first TSP that colonize the thymus were the only to generate $V\gamma5^+$ T cells (Ikuta et al., 1990; Ramond et al., 2013), it was important to determine whether they also generate thymic LTis, that together shape the thymic architecture (Roberts et al., 2012). Accordingly, ILC3 were the majority of embryonic thymic ILCs, gradually lost after birth, while a small population of ILC2 is maintained throughout life (Jones et al., 2018). It remained also to be determined whether the first wave of TSP are yolk sac (YS) or hematopoietic stem cell (HSC) derived. Addressing this question highlights a critical challenge in understanding T cell function.

Several successive but overlapping waves of emerging hematopoietic progenitors, with different lineage potential, are differentially regulated in time and space (Cumano and Godin, 2007; Perdiguero and Geissmann, 2016). Hematopoietic cells first appear in the extra-embryonic yolk sac (YS) blood islands at around embryonic day 7-7.5 (E7-7.5), where primitive erythropoiesis occurs prior to the emergence of multi-lineage erythro-myeloid

progenitors (EMPs) (Bertrand, 2005; Palis et al., 1999). The emergence of pre-HSCs starts at E9.5 in the aorta-gonad-mesonephros (AGM) and major arteries (Bertrand et al., 2010; Boisset et al., 2010; de Bruijn et al., 2000; Kissa and Herbomel, 2010), colonize the FL around E10.5 and later (around E16) migrate to the bone marrow (BM) (Cumano and Godin, 2007; Dzierzak and Bigas, 2018).

HSC are distinguished from all other progenitors by their ability to long-term repopulate all hematopoietic lineages (Cumano and Godin, 2007; Cumano et al., 2001). Emerging HSC cannot however be tested in assays similar to those used for adult HSC and are designated as pre-HSC (Cumano et al., 2001; Medvinsky and Dzierzak, 1996). Most hematopoietic cells are constantly differentiating from HSCs although a few lineages are HSC independent and exclusively produced during embryonic development. For example, YS cells that contribute to erythropoiesis and megakaryopoiesis are also the source of tissue resident macrophages that persist throughout life (Bertrand, 2005; Gomez Perdiguero et al., 2015a; Hoeffel et al., 2015; McGrath et al., 2015). This heterogeneity and layered organization of the hematopoietic system lead to the possibility that, similar to tissue macrophages, the first innate-like lymphocytes could also be YS derived. In line with this view, cells identified as lympho-myeloid restricted progenitors (LMPs) were observed in E9.5 YS before HSC activity is detected . They expressed lymphoid associated genes (*Il7r*, *Rag2*, *Rag1*) and were proposed as the origin of the first wave of TSP (Luis et al., 2016). Independent reports have also converged to support the notion that Vγ5$^+$ and another $\gamma\delta$ T cell subset, Vγ6$^+$ IL-17 producing might originate from YS progenitors, independent of HSCs (Gentek et al., 2018a; Spidale et al., 2018). In contrast to the above studies, Vγ5$^+$ and B1a B cells were shown to be preferentially derived from a particular HSC-like subset, transiently found in the FL but not in the adult BM, marked by an history of *Flk2* expression (Beaudin et al., 2016).

In this report, we undertook a characterization of the functional properties and fate of the progeny of the first TSP as well as their developmental origin. Unlike the current view that during embryogenesis ILCs are derived exclusively from the common α4β7$^+$ ILCs progenitors (Chea et al., 2016; De Obaldia and Bhandoola, 2015; Possot et al., 2011), we found that the first wave of TSP is composed of bipotent T/ILC progenitors that contribute to the thymic LTi cells, highlighting their unique and unprecedentedly reported role in generating ILC.

Moreover, the first TSP-derived conventional T cells that lack terminal deoxynucleotidyl transferase (TdT) expression and therefore exhibit a restricted T cell repertoire, are rapidly

overridden by subsequent waves of T cells. Therefore, the major role of the first wave of TSP might be restricted to provide cells that drive thymic organogenesis and homeostasis (Abramson and Anderson, 2017; Cumano et al., 2019; White et al., 2018). We further demonstrated for the first time *in vivo* that the embryonic TSPs are not YS-derived but rather originate from intra-embryonic HSCs. Interestingly, YS-derived progenitors although showing a history of lymphoid-associated gene expression, such as *Il7r*, *Rag2*, *Rag1*, did not differentiate into any lymphoid subset *in vivo* or *in vitro*. This transient expression, also found in other FL myeloid progenitors, is restricted to embryonic hematopoiesis and uncoupled from differentiation potential. Altogether our data highlight the impact of embryonic developmental timing on lymphocyte production, gene expression and the heterogeneity of the immune system.

RESULTS

Initial TSP show LTi biased lineage potential *in vitro*

A detailed analysis of the transcriptional profiles of TSP from the first (E13) and the second (E18) waves identified the overexpression, in the former, of ILC related transcripts from which stood out LTi-associated lineage transcripts (*Rorc*, *Cd4*, *Cxcr5*, *Il1r1* and *Ltb*) ;Supplementary Fig 1a) (Ishizuka et al., 2016; Ramond et al., 2013). This comparison also showed that genes involved γδ T cells development (*Bhlhe40*, *Cited4*, *B4galnt2*, *Tgm2* and *Txk*) were differentially expressed between E13 and E18 TSPs (Supplementary Fig 1a). Of note, *Sell* and *Ly6a* were upregulated in E18 TSP, in line with their resemblance to LMPPs (Berthault et al., 2017; Ramond et al., 2013). In addition, the E14 DN3 thymocytes were devoid of TdT activity (Supplementary Fig 1b) giving rise to T cells with a restricted T cell repertoire raising the possibility that they do not contribute to the adaptive T cell compartment, but rather to the innate-like T cell and ILC compartments.

To determine their developmental potential, we performed a two-step culture (Berthault et al., 2017; Luc et al., 2012) (Fig 1a) that allowed the generation of all major lymphoid lineages (T, B, ILC, NK) and myeloid cells from single progenitors (Fig 1b). Consistent with our previous observations showing that TSP before E15.5 are restricted lymphoid progenitors biased for T cell generation (Ramond et al., 2013), we found that E13 TSP only generated T cells and ILC whereas E18 TSPs retained B and myeloid potential. Most TSP gave rise to T and ILCs, although a few (6-15%) only generated T cells and none gave rise to ILC only. About 59% of the clones derived from E18 TSP generated all subsets of ILC and NK cells, whereas only 24% of E13 TSP showed that capacity, suggesting that the latter are more differentiated and restricted in their potential than the former (Fig 1b, c).

The most striking difference between the two subsets was that 22% of E13 TSP and none of the E18 TSP generated only ILC3 in addition to T cells (Fig 1c). These results indicated that mid gestation (E12.5-15.5) TSP appear LTi biased.

The initial TSP show LTi-associated gene expression

To understand the molecular basis of the ILC lineage potential differences between E13 and E18 TSP we analyzed by multiplex qRT-PCR, the expression of 41 lymphoid-associated genes in single cells. Unsupervised hierarchical clustering identified 4 distinct clusters (Fig 2). Cluster I comprised a majority of E18 TSP and showed no expression of ILC associated

transcripts, consistent with their capacity to generate all ILC populations. Clusters II and IV were essentially composed of E13 TSP and were characterized by the expression of common T/ILC genes *Tox*, *Tcf7* and *Gata3*. Cluster IV also expressed the LTi cell associated transcripts *Cxcr6*, *Cd4*, *Rorc*, *Cxcr5*, *Il1r1* and *Ltb*, consistent with their ILC3 restricted differentiation potential, whereas Cluster II expressed the innate-like T cells/ILC-associated transcripts *Zbtb16, Gzmb, Nfil3, Itga2b* and *Gzma* (De Obaldia and Bhandoola, 2015). Cluster III contained two thirds of E13 TSP and one third of E18 TSP and was characterized by the expression of low levels of *Tox*, *Gata3*, *Tcf7*, *Sox4*, *Runx1* and *Runx3* indicative of common T/ILC priming and consistent with a broad ILC differentiation potential (Fig1c).

Most TSP showed reduced signs of Notch signaling activation with few cells expressing *Hes1* consistent with their *in vitro* capacity to generate both T cells and ILC. This is in line with the observation that FL lymphoid progenitors expressed ILC associated transcripts before settling the thymus (Berthault et al., 2017; Possot et al., 2011).

Embryonic TSP have multi-ILC lineage potential *in vivo*

We next assessed the ILC lineage potential of E13 and E18 TSPs *in vivo.* CD45.2^{+} E13 or E18 ETPs were intravenously transferred into 1-day old Rag2$^{-/-}$γc$^{-/-}$ CD45.1^{+} mice. Recipient mice were analyzed at 5 weeks post-transfer (Fig. 3a). While mice engrafted with E13 TSP only generated ILC, E18 TSP also generated B and myeloid cells, (Fig 3b; supplementary Fig 2b,c) consistent with the more restricted differentiation potential of E13 TSP. As expected, few T cells were generated in these chimeras because of the atrophic thymus in Rag2$^{-/-}$γc$^{-/-}$ mice and because TSP down-regulate Ccr7 and Ccr9 as they enter the thymus and consequently lose their ability to home back to the thymus (Zlotoff et al., 2010).

Analysis of intestinal lamina propria, where all ILC lineages coexist, showed that TSP from both waves generated NK cells (EOMES^{+}), ILC1 (EOMES^{-}), ILC3 (RORγt^{+}) and ILC2 (GATA3^{+}). In the lung we found ILC2, in the spleen NK cells and in the liver NK cells and ILC1 (Fig 3c,d; supplementary Fig 2a). These results indicated that E13 and E18 TSP have the capacity to generate all ILC subsets *in vivo* and that the ILC generated recapitulated the expected tissue distribution.

Neonatal thymectomy has no effect on tissue colonization by embryonic derived Vγ5$^+$ and Vγ6$^+$ γδ T cells

Vγ5$^+$ and Vγ6$^+$ γδ T cells in the skin and in the lymph nodes (LN), respectively, are of embryonic origin (Haas et al., 2012; Ikuta et al., 1990). To assess the dependency of these embryonic tissue resident γδ T subsets on thymic output that might inform on their origin in the first or second wave of TSP, we performed neonatal thymectomy. Newborn (up to 36 hours after birth) mice were thymectomized or sham-operated as a control (Fig 4a). At 6 weeks of age complete thymectomy was ascertained by the absence of double positive CD4/CD8 cells in the tissue around the thymus location (Fig 4b). Thymectomized mice (n=6) were severely lymphopenic as shown by the numbers of CD4 and CD8 αβ T cells in the inguinal (i) LN (Fig 4d) and in the spleen; of note, CD44$^-$ αβ T cells in the spleen were severely reduced (Fig 4e), a sign of activation of the T cell compartment consequent to the lymphopenia and consistent with the absence of a functional thymus in these mice. By contrast, the numbers of Vγ5$^+$ γδ T cells in the skin and those of Vγ4$^-$ IL17$^+$ γδ T cells (considered as Vγ6$^+$ γδ T) in the iLN were similar in sham and in thymectomized animals (Fig 4c, d). By contrast, iLN Vγ4$^+$ IL17$^+$ γδ T cells were severely reduced (Fig 4d). These experiments suggest that the two embryonic γδ T cell subsets are likely derived from the first wave of TSP. All other αβ or γδ T depend on post-natal thymic output and thus are likely largely issued from the second wave of TSP.

E9.5 YFP expressing *Il7rα*^{Cre}Rosa26^{YFP} YS-progenitors are devoid of lymphoid potential

The experiments above indicated that the first cells that colonize the thymus are particularly efficient in generating ILC and embryonic γδ T cells. Because YS derived progenitors express lymphoid associated genes such as *Rag*, *Flt3* and *Il7r* (Böiers et al., 2013; Luis et al., 2016) we considered the possibility that the first TSP originated in an HSC independent pathway. This notion was further reinforced by a recent report suggesting a YS origin of Vγ5$^+$ γδ T (Gentek et al., 2018a).

We used a lineage tracer mouse line to identify the onset of *Il7r*-expressing cells, *Il7rα*^{Cre}Rosa26^{YFP} (Schlenner et al., 2010). We performed time course analyses of YFP expressing cells in the YS, head, AGM region and FL (Fig 5a). No YFP expression was observed in E8.5 embryos, in any of the analyzed tissues in either the Kit$^+$ or Kit$^-$ fraction (data not

shown). Consistent with previous studies, YFP$^+$ progenitors were first detected in Lin$^-$ Kit$^+$CD41$^+$ YS cells and were undetected in the AGM or in the placenta (Fig 5d) at E9.5 in *Il7ra*^{Cre}Rosa26^{YFP} embryos (Fig 5b,c). 5-8 % of the c-kit$^+$ cells in the YS were YFP$^+$ (Fig 5b,c), also expressed CD31 and CD16/32 and lacked surface expression of CD135, CD127 or CD115 (Fig 5e), the phenotype of YS EMPs (Bertrand, 2005; McGrath et al., 2015).

To further investigate the potential of YS YFP$^+$ cells to develop into T/GM and B/GM cells, single cells were cultured into monolayers of OP9-DL4 or OP9 stroma (Fig 5f). YFP$^+$ YS cells showed myeloid potential and lacked detectable T or B cell potential (Fig 5g, h). Methylcellulose-based colony assays showed that both Lin$^-$Kit$^+$YFP$^+$ and Lin$^-$Kit$^+$YFP$^-$ YS cells exhibited comparable GM and MkE potential (Fig 5i). These results indicated that expression of YFP in the E9.5 YS *Il7ra*^{Cre}Rosa26^{YFP} embryos does not equate with lymphoid potential, and that both YFP$^+$ and YFP$^-$ E9.5 YS Kit$^+$ cells showed a lineage potential similar to erythro-myeloid progenitors (EMPs) (Bertrand, 2005; Gomez Perdiguero et al., 2015a; McGrath et al., 2015).

To determine whether E9.5 YS Kit$^+$ progenitors could give rise to the first differentiating $\gamma\delta$ T cells, the Vγ5$^+$ T cells, we performed FTOC of thymic lobes colonized with either E9.5 YS Kit$^+$ YFP$^+$ progenitors, E10.5 YS-Kit$^+$ progenitors or E12 FL LSKs as a control (Fig 5j). Consistent with their inability to generate T cells in OP9-DL4 cultures, E9.5 YS-derived cells did not generate Vγ5$^+$ T cells or initiate thymopoiesis. By contrast, E10.5 YS-Kit$^+$ progenitors and E12 FL LSK readily generated T cells including Vγ5$^+$ T cells. E10.5 YS-Kit$^+$ progenitor derived T cells originate from AGM-derived pre-HSC, known to enter circulation between E9.5 and E11.5 (Delassus and Cumano, 1996; McGrath et al., 2003) and were used to probe the sensitivity of the T cell assay. These experiments showed that E9.5 YS progenitors are devoid of lymphoid potential under culture conditions sufficiently sensitive to detect few circulating T cell progenitors.

Expression of *Il7r* and *Flk2* in YFP$^+$ E9.5 IL7r^{Cre}Rosa^{YFP} YS progenitors is transient

To better characterize YFP$^+$ YS progenitors, which share phenotype and differentiation potential with EMPs, we analyzed the expression of transcripts associated with multiple hematopoietic lineages in single E9.5 YS YFP$^+$ and YFP$^-$ Lin$^-$ CD117$^+$ CD41$^+$ cells. Unsupervised hierarchical clustering segregate YFP$^+$ and YFP$^-$ cells into four clusters (Supplementary Fig 3a). Clusters I and II, comprises mostly YFP+ cells and are characterized by the expression of

Pu-1, *Irf8 Csf1r* a pattern of expression corresponding to EMPs (Mass et al., 2016) (Supplementary Fig 3b). Cluster II and a fraction of cluster I showed also expression of ,*Kdr*, *Tek*, *Runx1*, *Mpl* and *Foxo1*, suggesting that they were EMP recently specified from hemogenic endothelium (Baron et al., 2018; Kasaai et al., 2017; Mass et al., 2016). Furthermore, cells in cluster II also expressed the lymphoid-associated genes *Il7ra* and *Flk2*. Clusters III and IV comprised both YFP$^-$ and YFP$^+$ cells expressing high levels of *Gata1* indicating their erythroid lineage engagement and did not express any of the lymphoid genes. Cells in cluster IV also expressed *Klf1* indicating that they are more advanced into the erythroid lineage differentiation. *Ebf1*, *Pax5* or *Rag1* were not detected in any YS cells

Quantitative PCR performed on bulk populations showed that YFP$^+$ cells expressed significantly higher levels of *Rag1*, *Rag2* and *Il7r* than YFP$^-$ cells albeit 10-fold lower than CLP (Supplementary Fig 4). Altogether, these experiments indicated that the transient lymphoid associated gene expression in YS cells is restricted to the more immature cells, i.e. the emerging YS-derived EMP and is dissociated from their differentiation potential.

FL myeloid progenitors are labelled in *Il7ra*^{Cre}Rosa26^{YFP} mouse embryos.

To study the possibility that YS derived progenitors contribute to the lymphoid lineage during embryogenesis *in vivo*, we mapped YFP$^+$ cells in *Il7ra*^{Cre}Rosa26^{YFP} mice. We found that, unlike in adult BM where *Il7r*^{Cre} labels exclusively lymphoid progenitors (Schlenner et al., 2010), YFP expression in the FL was also found in multipotent and myeloid progenitors (Supplementary Fig 5a,b). FL and fetal blood (FB), short-term HSCs (ST-HSCs), multipotent progenitors (MPPs), granulocytes-myeloid progenitors (GMPs), common myeloid progenitors (CMPs) and megakaryocytes-erythroid progenitors (MEPs) were labeled at frequencies ranging from 10%-40% (Supplementary Fig 5a,b; see Supplementary Figure 6 for gating strategy). The frequency of YFP$^+$ ST-HSC and myeloid progenitors progressively decreased after birth and was undetectable in adult mice (Schlenner et al., 2010) (Supplementary Fig 5b). FL YFP$^+$ GMPs and CMPs lacked any detectable B cell potential *in vitro*, retaining GM potential (Supplementary Fig 5c). These observations indicated that at early stages of development *Il7ra*^{Cre} also labels cells devoid of lymphoid potential, and therefore this model does not faithfully trace the origin of embryonic lymphoid cells.

To establish whether YFP$^+$ cells contribute to tissue-specific hematopoietic lineages known to be of embryonic origin (Gentek et al., 2018b; Gomez Perdiguero et al., 2015b) we analyzed

the brain microglia, the FL Kupffer cells and the skin mast and Langerhans cells of E18 *Il7ra*^{Cre}Rosa26^{YFP}. We found expression of YFP in about 40% of all these populations (Supplementary Fig 7a, b).

Thymopoiesis-initiating cells develop exclusively from HSC-derived progenitors

To define the relative contribution of YS cells and HSCs to the first wave of TSPs, we used a fate mapping mouse model expressing the tamoxifen inducible Cre (*MeriCreMer*) under the control of the *Csf1r* promoter (Qian et al., 2011) (Fig 6a). We crossed *Csf1r*^{MeriCreMer} mice with the Cre reporter mouse strain *Rosa26*^{YFP} or *Rosa26*^{Tomato} (based on the availability of fluorochrome-labelled antibodies for the analysis) and induced recombination in embryos by a single injection of Hydroxytamoxifen (4-OH-TAM) into E8.5, E9.5 or E10.5 pregnant females. *Csf1r* is first expressed in E8.5 YS progenitors (Gomez Perdiguero et al., 2015a), later it is expressed in E9.5 YS *Il7ra*^{Cre}Rosa26^{YFP} (Supplementary Fig 3) (Böiers et al., 2013) and at E10.5 *Csf1r* is also expressed in pre-HSC (Baron et al., 2018) (Supplementary Fig 8d). Consequently, single 4-OH-TAM injection at E8.5 or E9.5 should mark *Csf1r*-expressing myeloid cells and EMP of YS origin that also comprise *Il7r* traced cells. Injection of 4-OH-TAM at E10.5 should mark HSC derived progenitors and *Csf1r*-expressing myeloid cells.

In embryos pulsed at E8.5, YFP$^+$ cells were detected in the E9.5 YS. These cells expressed *Csf1r*, *Il7r* and were devoid of lymphoid potential (Supplementary Fig 8a,b,c). In embryos pulsed at either E8.5 or E9.5 and analyzed at E12.5, YFP$^+$ HSC, HSC-derived lymphoid progenitors and TSP were either not detectable or represented less than 1% in FL and thymus, respectively (Fig 6b,c). In contrast, 30-50% of microglia cells were labeled, in line with their YS origin. Embryos pulsed at E10.5 and analyzed at E12.5 showed significant labeling in populations of FL HSC, multipotent, lymphoid and myeloid progenitors (Fig 6c). Interestingly, the frequency of Tomato$^+$ cells in E12.5 TSP (25%) and in FL LTi (22%) (See supplementary Fig 8e for gating strategy) paralleled that of HSCs (31%).

These fate-mapping experiments directly demonstrated that no detectable TSP and lymphoid progenitor originate from YS cells under physiological conditions; rather their origin coincides in time with that of pre-HSC.

Innate-like Vγ5$^+$ T cells or B1-a cells that differentiate during a limited time window of embryonic development have been proposed to derive from HSC-independent precursors (Gentek et al., 2018a; Ghosn et al., 2016). Therefore, we analyzed Vγ5$^+$ T cells and B-1a in the

skin and peritoneal cavity respectively of adult *Csf1r*^{MeriCreMer} *Rosa26*^{YFP} or *Csf1r*^{MeriCreMer} *Rosa26*^{Tomato} mice pulsed at either E8.5, E9.5 or E10.5 (See supplementary Fig 8f for gating strategy).

Adult mice pulsed at E8.5 showed no YFP labelled lymphocytes and those pulsed at E9.5 showed less than 1% of Vγ5^{+} T or B-1a labelled cells, while 30-40% of microglia cells were YFP labelled (Fig 6c). By contrast, embryos pulsed at E10.5 showed frequencies of Vγ5^{+} T or B-1a labelled cells similar to that found in HSCs (Fig 6c). These results are consistent with a strict HSC origin of all lymphoid cells including the first wave of TSP and innate-like lymphocytes of embryonic origin.

DISSCUSION

Here we show that the first wave of embryonic TSP developed exclusively from HSC and show a unique capacity to generate LTi and Vγ5$^+$ $\gamma\delta$ T cells that, together, shape the thymic architecture.

The interaction between the first developing Vγ5$^+$ T cells and CD4$^+$ CD3$^-$ LTi with thymic medullary epithelial cells, results in the expression of Aire by the latter, which is essential to establish thymic T cell tolerance (Abramson and Anderson, 2017; Roberts et al., 2012; Rossi et al., 2007). We have previously shown that the first TSP derive from a unique and transient set of hematopoietic progenitors, T-biased in their differentiation potential, that colonize the thymus between E12.5 and E15.5 (Berthault et al., 2017; Ramond et al., 2013) . These precursors were the only capable of generating Vγ5$^+$ $\gamma\delta$ T cells (Ramond et al., 2013). We show here, by single cell lineage potential assays, that these TSP comprise a population restricted to the T and ILC3 lineages. This observation was further supported by transcriptional analyses showing a cluster of E13.5 TSP that, although not committed, are primed and biased towards the ILC3 lineage with high expression of *Rorc*, *Cd4*, *Cxcr5*, *Il1r1* and *Ltb*, a signature of LTi (Ishizuka et al., 2016; Kernfeld et al., 2018). Together with the lack of detectable ILC restricted progenitors within E13.5 thymocytes and the temporally linked appearance of thymic LTi and Aire$^+$ mTECs (Rossi et al., 2007), these results indicate that the first TSP contribute to both Vγ5 T cells and thymic LTi and are therefore the main actors in shaping thymic architecture.

The first TSP were also devoid of TdT activity giving rise to T cells without N sequences and thus with a restricted T cell repertoire. Low TdT expression together with the poor proliferative capacity and the observation that after P4 virtually all $\alpha\beta$ expressing conventional T cells have N sequences in their V(D)J junctions (Bogue et al., 1992), suggested that the contribution of the first TSP to the conventional T cell compartment is limited (Cumano et al., 2019).

In vivo TSP were capable of restoring the tissue resident ILC compartments of newborn Rag2γc$^{-/-}$ mice. This finding suggests that TSP in circulation can home to the peripheral tissues and differentiate *in situ* into all ILC populations.

Our data show that the first TSP isolated using generally accepted markers (Porritt et al., 2004; Ramond et al., 2013) are T/ILC restricted with poor B and myeloid potential arguing against the notion that the embryonic thymus is initially seeded by lympho-myeloid

restricted progenitors. Using *Rag1*-GFP mice, it was argued that E11.5 TSP retained myeloid potential and resembled PIRA/B$^+$ LMPPs in phenotype, lineage potential and molecular signature (Luis et al., 2016). However, it is not clear whether these cells were TSP because, at this stage, the epithelium that forms the thymus anlage is not yet folded resulting in a difficult distinction from the surrounding pharyngeal pouches. Moreover, the analysis based on the unique expression of GFP might include a heterogeneous population of circulating hematopoietic progenitors, thus compromising the conclusions from this study. Different strategies to isolate TSP might explain the discrepancies in lineage potential and molecular signature between the two studies.

As the origin of progenitors during development may be linked to the generation of distinct populations within the immune system, we revisited the controversial origin of the first wave of TSP. By analogy with the documented YS origin of tissue resident macrophages (Gomez Perdiguero et al., 2015b; Perdiguero and Geissmann, 2016), it was proposed that also early developing innate-like T cells and therefore the first TSP were HSC independent (Böiers et al., 2013; Gentek et al., 2018a; Kobayashi et al., 2014; Luis et al., 2016; Spidale et al., 2018; Yoshimoto et al., 2011, 2012).

The evidence that YS is a potential source of early lymphocytes is based on adoptive transfer experiments, on mice that lack blood circulation or by tracing YS cells expressing lymphoid-associated genes (Böiers et al., 2013; Yoshimoto et al., 2012). The complexity of hematopoietic cell generation that occurs in multiple sites in overlapping time windows hampers the precise assignment of hematopoietic progenitor origin. To unambiguously assign the contribution of each anatomical site to blood cell formation, faithful lineage tracing models that trace the progeny of each source in a non-overlapping spatio-temporal manner have to be used.

Our analysis of YFP expressing cells under the control of the *Il7r* regulatory sequences throughout embryonic life indicated that, unlike adult hematopoietic progenitors, multipotent and myeloid restricted embryonic progenitors express lymphoid associated genes, albeit in a transient manner, without any consequent restriction in their differentiation potential. Consistent with our analysis, a recent report using the same mouse model demonstrated that FL hematopoietic progenitors and tissue resident macrophages were significantly labeled (Gautier et al., 2012; Heng et al., 2008; Leung et al., 2019). These

observations established that in hematopoiesis, gene expression does not necessarily equate with lineage potential.

The analyses of inducible lineage tracing of *Cdh5* and *Runx1* expressing cells (Gentek et al., 2018a) suggested that Vγ5$^+$ T cells were generated from early emerging hematopoietic cells, precisely from YS-derived hematopoietic progenitors. Because *Cdh5* and *Runx1* are expressed in both endothelial and hematopoietic cells these models do not allow a clear discrimination between progenitors originated in the YS or in the dorsal aorta. Moreover, the lack of direct comparison between the labeling efficiency in HSC and in Vγ5$^+$ T cells compromise the conclusions obtained from these mouse models.

Csf1r^{MerCreMer} lineage tracing allowed a temporal analysis and unambiguously traced YS derived progenitors (including those expressing lymphoid-associated genes) in females induced at E8.5 and E9.5, while it traced both HSC and YS derived *Csf1r* expressing myeloid cells, when pulsed at E10.5.

Microglia but virtually no HSC, Vγ5$^+$ $\gamma\delta$ T cells or B1a B cells were labeled by a single pulse at E8.5. In contrast, induction at E10.5 labelled HSC, Vγ5+ T cells and B1a B cells with similar efficiencies, indicating a lineage relationship. Moreover, when pulsed at E9.5 a low (less than 1%) frequency of labelled HSC was accompanied by equally low frequency of labelled innate-like lymphocytes. These fate mapping experiments are the first *in vivo* evidence that directly demonstrate that TSPs, innate-like lymphocytes and lymphoid progenitors originate in the embryo from *Csf1r*$^+$ HSCs-derived progeny, show no contribution of HSC-independent progenitors to lymphopoiesis and settle the controversy over the lymphoid ontogeny during embryogenesis. Together these data indicate that lymphopoiesis is a hallmark of HSC and HSC-derived progenitors

The existence of restricted lymphoid progenitors in the FL between E11.5 to E15.5 suggests that the generation of embryonic-derived tissue resident lymphoid cells follows a unique developmental program. These cells are produced prior to the establishment of a fully competent adaptive immunity and persist throughout life, that possibly contribute to the integrity of body barriers and act as a first line of defense against pathogens. The ability of embryonic TSP to generate ILCs is the first evidence that they can originate also from hematopoietic progenitors other than the classical ILCP, and in organs other than the FL where hematopoiesis occurs (Fig 7). This highly orchestrated sequence of events highlights

the requirement of a layered immune cell production whereby the first wave of TSPs is essential for thymic organogenesis and homeostasis.

ACKNOWLEDGMENTS

We thank S. Novault, S. Megharba and S. Schmutz from the flow cytometry core facility of the Institut Pasteur for technical support; the staff of the animal facility of the Institut Pasteur for mouse care. We thank H.-R. Rodewald for providing *Il7ra*^{Cre}Rosa26^{YFP} mice and S.E.W. Jacobsen for fruitful discussions. This work was financed by the Institut Pasteur, INSERM, Pasteur-Weizmann Foundation and ANR (grant Twothyme) through grants to A.C.; by REVIVE (Investissement d'Avenir; ANR-10-LABX-73) to A.C. and R.E.; by recurrent funding from the Institut Pasteur, the CNRS, Revive (Investissement d'Avenir; ANR-10-LABX-73) and by an ERC investigator award (2016-StG-715320) from the European Research Council to E.G.P.

AUTHOR CONTRIBUTIONS

R.E. designed and performed most experiments, analyzed data and wrote the manuscript; S.M. analyzed chimeric mice and contributed to discussions. F.S.S. and T.P. performed Biomark analysis. O.B.-D performed neonatal thymectomy. E.G.P., L.F. and L.I. performed fate-mapping experiments. A.B. performed adoptive transfer in neonatal mice. R.G., P.V., A.B. and P.P. contributed to the discussions. A.C. directed the research, designed experiments, analyzed data and wrote the manuscript. All authors contributed to the manuscript.

COMPETING FINANCIAL INTERESTS

The authors declare no competing financial interests.

REFERENCES

Abramson, J., and Anderson, G. (2017). Thymic Epithelial Cells. Annu. Rev. Immunol. *35*, 85–118.

Alves, N.L., Takahama, Y., Ohigashi, I., Ribeiro, A.R., Baik, S., Anderson, G., and Jenkinson, W.E. (2014). Serial progression of cortical and medullary thymic epithelial microenvironments. Eur. J. Immunol. *44*, 16–22.

Baron, C.S., Kester, L., Klaus, A., Boisset, J.-C., Thambyrajah, R., Yvernogeau, L., Kouskoff, V., Lacaud, G., van Oudenaarden, A., and Robin, C. (2018). Single-cell transcriptomics reveal the dynamic of haematopoietic stem cell production in the aorta. Nat. Commun. *9*.

Beaudin, A.E., Boyer, S.W., Perez-Cunningham, J., Hernandez, G.E., Derderian, S.C., Jujjavarapu, C., Aaserude, E., MacKenzie, T., and Forsberg, E.C. (2016). A Transient Developmental Hematopoietic Stem Cell Gives Rise to Innate-like B and T Cells. Cell Stem Cell *19*, 768–783.

Berthault, C., Ramond, C., Burlen-Defranoux, O., Soubigou, G., Chea, S., Golub, R., Pereira, P., Vieira, P., and Cumano, A. (2017). Asynchronous lineage priming determines commitment to T cell and B cell lineages in fetal liver. Nat. Immunol. *18*, 1139–1149.

Bertrand, J.Y. (2005). Three pathways to mature macrophages in the early mouse yolk sac. Blood *106*, 3004–3011.

Bertrand, J.Y., Chi, N.C., Santoso, B., Teng, S., Stainier, D.Y.R., and Traver, D. (2010). Hematopoietic stem cells derive directly from aortic endothelium during development. Nature *464*, 108–111.

Bhandoola, A., von Boehmer, H., Petrie, H.T., and Zúñiga-Pflücker, J.C. (2007). Commitment and Developmental Potential of Extrathymic and Intrathymic T Cell Precursors: Plenty to Choose from. Immunity *26*, 678–689.

Bogue, M., Gilfillan, S., Benoist, C., and Mathis, D. (1992). Regulation of N-Region Diversity in Antigen Receptors Through Thymocyte Differentiation and Thymus Ontogeny. Proc. Natl. Acad. Sci. U. S. A. *89*, 11011–11015.

Böiers, C., Carrelha, J., Lutteropp, M., Luc, S., Green, J.C.A., Azzoni, E., Woll, P.S., Mead, A.J., Hultquist, A., Swiers, G., et al. (2013). Lymphomyeloid Contribution of an Immune-Restricted Progenitor Emerging Prior to Definitive Hematopoietic Stem Cells. Cell Stem Cell *13*, 535–548.

Boisset, J.-C., van Cappellen, W., Andrieu-Soler, C., Galjart, N., Dzierzak, E., and Robin, C.

(2010). In vivo imaging of haematopoietic cells emerging from the mouse aortic endothelium. Nature *464*, 116–120.

Boyden, L.M., Lewis, J.M., Barbee, S.D., Bas, A., Girardi, M., Hayday, A.C., Tigelaar, R.E., and Lifton, R.P. (2008). Skint1, the prototype of a newly identified immunoglobulin superfamily gene cluster, positively selects epidermal gammadelta T cells. Nat. Genet. *40*, 656–662.

de Bruijn, M.F.T.R., Speck, N.A., Peeters, M.C.E., and Dzierzak, E. (2000). Definitive hematopoietic stem cells first develop within the major arterial regions of the mouse embryo. EMBO J. *19*, 2465–2474.

Cumano, A., and Godin, I. (2007). Ontogeny of the Hematopoietic System. Annu. Rev. Immunol. *25*, 745–785.

Cumano, A., Ferraz, J.C., Klaine, M., Di Santo, J.P., and Godin, I. (2001). Intraembryonic, but Not Yolk Sac Hematopoietic Precursors, Isolated before Circulation, Provide Long-Term Multilineage Reconstitution. Immunity *15*, 477–485.

Cumano, A., Berthault, C., Ramond, C., Petit, M., Golub, R., Bandeira, A., and Pereira, P. (2019). New Molecular Insights into Immune Cell Development. Annu. Rev. Immunol. *37*, 497–519.

Cupedo, T., and Mebius, R.E. (2003). Role of chemokines in the development of secondary and tertiary lymphoid tissues. Semin. Immunol. *15*, 243–248.

Cupedo, T., Kraal, G., and Mebius, R.E. (2002). The role of CD45+CD4+CD3- cells in lymphoid organ development. Immunol. Rev. *189*, 41–50.

De Obaldia, M.E., and Bhandoola, A. (2015). Transcriptional Regulation of Innate and Adaptive Lymphocyte Lineages. Annu. Rev. Immunol. *33*, 607–642.

Delassus, S., and Cumano, A. (1996). Circulation of Hematopoietic Progenitors in the Mouse Embryo. Immunity *4*, 97–106.

Dzierzak, E., and Bigas, A. (2018). Blood Development: Hematopoietic Stem Cell Dependence and Independence. Cell Stem Cell *22*, 639–651.

Gautier, E.L., Shay, T., Miller, J., Greter, M., Jakubzick, C., Ivanov, S., Helft, J., Chow, A., Elpek, K.G., Gordonov, S., et al. (2012). Gene-expression profiles and transcriptional regulatory pathways that underlie the identity and diversity of mouse tissue macrophages. Nat. Immunol. *13*, 1118–1128.

Gentek, R., Ghigo, C., Hoeffel, G., Jorquera, A., Msallam, R., Wienert, S., Klauschen, F., Ginhoux, F., and Bajénoff, M. (2018). Epidermal γδ T cells originate from yolk sac hematopoiesis and clonally self-renew in the adult. J. Exp. Med. *215*, 2994–3005.

Gomez Perdiguero, E., Klapproth, K., Schulz, C., Busch, K., Azzoni, E., Crozet, L., Garner,

H., Trouillet, C., de Bruijn, M.F., Geissmann, F., et al. (2015a). Tissue-resident macrophages originate from yolk-sac-derived erythro-myeloid progenitors. Nature *518*, 547–551.

Gomez Perdiguero, E., Klapproth, K., Schulz, C., Busch, K., Azzoni, E., Crozet, L., Garner, H., Trouillet, C., de Bruijn, M.F., Geissmann, F., et al. (2015b). Tissue-resident macrophages originate from yolk-sac-derived erythro-myeloid progenitors. Nature *518*, 547–551.

Haas, J.D., Ravens, S., Düber, S., Sandrock, I., Oberdörfer, L., Kashani, E., Chennupati, V., Föhse, L., Naumann, R., Weiss, S., et al. (2012). Development of Interleukin-17-Producing γδ T Cells Is Restricted to a Functional Embryonic Wave. Immunity *37*, 48–59.

Heng, T.S.P., Painter, M.W., and Immunological Genome Project Consortium (2008). The Immunological Genome Project: networks of gene expression in immune cells. Nat. Immunol. *9*, 1091–1094.

Hoeffel, G., Chen, J., Lavin, Y., Low, D., Almeida, F.F., See, P., Beaudin, A.E., Lum, J., Low, I., Forsberg, E.C., et al. (2015). C-Myb+ Erythro-Myeloid Progenitor-Derived Fetal Monocytes Give Rise to Adult Tissue-Resident Macrophages. Immunity *42*, 665–678.

Ikuta, K., Kina, T., MacNeil, I., Uchida, N., Peault, B., Chien, Y.H., and Weissman, I.L. (1990). A developmental switch in thymic lymphocyte maturation potential occurs at the level of hematopoietic stem cells. Cell *62*, 863–874.

Ishizuka, I.E., Chea, S., Gudjonson, H., Constantinides, M.G., Dinner, A.R., Bendelac, A., and Golub, R. (2016). Single-cell analysis defines the divergence between the innate lymphoid cell lineage and lymphoid tissue–inducer cell lineage. Nat. Immunol. *17*, 269–276.

Jones, R., Cosway, E.J., Willis, C., White, A.J., Jenkinson, W.E., Fehling, H.J., Anderson, G., and Withers, D.R. (2018). Dynamic changes in intrathymic ILC populations during murine neonatal development. Eur. J. Immunol. *48*, 1481–1491.

Kasaai, B., Caolo, V., Peacock, H.M., Lehoux, S., Gomez-Perdiguero, E., Luttun, A., and Jones, E.A.V. (2017). Erythro-myeloid progenitors can differentiate from endothelial cells and modulate embryonic vascular remodeling. Sci. Rep. *7*, 43817.

Kernfeld, E.M., Genga, R.M.J., Neherin, K., Magaletta, M.E., Xu, P., and Maehr, R. (2018). A Single-Cell Transcriptomic Atlas of Thymus Organogenesis Resolves Cell Types and Developmental Maturation. Immunity *48*, 1258-1270.e6.

Kissa, K., and Herbomel, P. (2010). Blood stem cells emerge from aortic endothelium by a novel type of cell transition. Nature *464*, 112–115.

Kobayashi, M., Shelley, W.C., Seo, W., Vemula, S., Lin, Y., Liu, Y., Kapur, R., Taniuchi, I., and Yoshimoto, M. (2014). Functional B-1 progenitor cells are present in the hematopoietic stem cell-deficient embryo and depend on Cbf for their development. Proc. Natl. Acad. Sci. *111*, 12151–12156.

Leung, G.A., Cool, T., Valencia, C.H., Worthington, A., Beaudin, A.E., and Forsberg, E.C. (2019). The lymphoid-associated interleukin 7 receptor (IL7R) regulates tissue-resident macrophage development. Dev. Camb. Engl. *146*.

Luc, S., Luis, T.C., Boukarabila, H., Macaulay, I.C., Buza-Vidas, N., Bouriez-Jones, T., Lutteropp, M., Woll, P.S., Loughran, S.J., Mead, A.J., et al. (2012). The earliest thymic T cell progenitors sustain B cell and myeloid lineage potential. Nat. Immunol. *13*, 412–419.

Luis, T.C., Luc, S., Mizukami, T., Boukarabila, H., Thongjuea, S., Woll, P.S., Azzoni, E., Giustacchini, A., Lutteropp, M., Bouriez-Jones, T., et al. (2016). Initial seeding of the embryonic thymus by immune-restricted lympho-myeloid progenitors. Nat. Immunol. *17*, 1424–1435.

Mass, E., Ballesteros, I., Farlik, M., Halbritter, F., Günther, P., Crozet, L., Jacome-Galarza, C.E., Händler, K., Klughammer, J., Kobayashi, Y., et al. (2016). Specification of tissue-resident macrophages during organogenesis. Science *353*.

McGrath, K.E., Koniski, A.D., Malik, J., and Palis, J. (2003). Circulation is established in a stepwise pattern in the mammalian embryo. Blood *101*, 1669–1675.

McGrath, K.E., Frame, J.M., Fegan, K.H., Bowen, J.R., Conway, S.J., Catherman, S.C., Kingsley, P.D., Koniski, A.D., and Palis, J. (2015). Distinct Sources of Hematopoietic Progenitors Emerge before HSCs and Provide Functional Blood Cells in the Mammalian Embryo. Cell Rep. *11*, 1892–1904.

Medvinsky, A., and Dzierzak, E. (1996). Definitive Hematopoiesis Is Autonomously Initiated by the AGM Region. Cell *86*, 897–906.

Palis, J., Robertson, S., Kennedy, M., Wall, C., and Keller, G. (1999). Development of erythroid and myeloid progenitors in the yolk sac and embryo proper of the mouse. Dev. Camb. Engl. *126*, 5073–5084.

Papotto, P.H., Ribot, J.C., and Silva-Santos, B. (2017). IL-17+ γδ T cells as kick-starters of inflammation. Nat. Immunol. *18*, 604–611.

Perdiguero, E.G., and Geissmann, F. (2016). The development and maintenance of resident macrophages. Nat. Immunol. *17*, 2–8.

Porritt, H.E., Rumfelt, L.L., Tabrizifard, S., Schmitt, T.M., Zúñiga-Pflücker, J.C., and Petrie, H.T. (2004). Heterogeneity among DN1 Prothymocytes Reveals Multiple Progenitors with Different Capacities to Generate T Cell and Non-T Cell Lineages. Immunity *20*, 735–745.

Possot, C., Schmutz, S., Chea, S., Boucontet, L., Louise, A., Cumano, A., and Golub, R. (2011). Notch signaling is necessary for adult, but not fetal, development of RORγt(+) innate lymphoid cells. Nat. Immunol. *12*, 949–958.

Qian, B.-Z., Li, J., Zhang, H., Kitamura, T., Zhang, J., Campion, L.R., Kaiser, E.A., Snyder,

L.A., and Pollard, J.W. (2011). CCL2 recruits inflammatory monocytes to facilitate breast-tumour metastasis. Nature *475*, 222–225.

Ramond, C., Berthault, C., Burlen-Defranoux, O., de Sousa, A.P., Guy-Grand, D., Vieira, P., Pereira, P., and Cumano, A. (2013). Two waves of distinct hematopoietic progenitor cells colonize the fetal thymus. Nat. Immunol. *15*, 27–35.

Roberts, N.A., White, A.J., Jenkinson, W.E., Turchinovich, G., Nakamura, K., Withers, D.R., McConnell, F.M., Desanti, G.E., Benezech, C., Parnell, S.M., et al. (2012). Rank signaling links the development of invariant γδ T cell progenitors and Aire(+) medullary epithelium. Immunity *36*, 427–437.

Rossi, S.W., Kim, M.-Y., Leibbrandt, A., Parnell, S.M., Jenkinson, W.E., Glanville, S.H., McConnell, F.M., Scott, H.S., Penninger, J.M., Jenkinson, E.J., et al. (2007). RANK signals from CD4+3− inducer cells regulate development of Aire-expressing epithelial cells in the thymic medulla. J. Exp. Med. *204*, 1267–1272.

Schlenner, S.M., Madan, V., Busch, K., Tietz, A., Läufle, C., Costa, C., Blum, C., Fehling, H.J., and Rodewald, H.-R. (2010). Fate Mapping Reveals Separate Origins of T Cells and Myeloid Lineages in the Thymus. Immunity *32*, 426–436.

Spidale, N.A., Sylvia, K., Narayan, K., Miu, B., Frascoli, M., Melichar, H.J., Zhihao, W., Kisielow, J., Palin, A., Serwold, T., et al. (2018). Interleukin-17-Producing γδ T Cells Originate from SOX13+ Progenitors that Are Independent of γδTCR Signaling. Immunity *49*, 857-872.e5.

White, A.J., Lucas, B., Jenkinson, W.E., and Anderson, G. (2018). Invariant NKT Cells and Control of the Thymus Medulla. J. Immunol. Baltim. Md 1950 *200*, 3333–3339.

Yoshimoto, M., Montecino-Rodriguez, E., Ferkowicz, M.J., Porayette, P., Shelley, W.C., Conway, S.J., Dorshkind, K., and Yoder, M.C. (2011). Embryonic day 9 yolk sac and intra-embryonic hemogenic endothelium independently generate a B-1 and marginal zone progenitor lacking B-2 potential. Proc. Natl. Acad. Sci. U. S. A. *108*, 1468–1473.

Yoshimoto, M., Porayette, P., Glosson, N.L., Conway, S.J., Carlesso, N., Cardoso, A.A., Kaplan, M.H., and Yoder, M.C. (2012). Autonomous murine T-cell progenitor production in the extra-embryonic yolk sac before HSC emergence. Blood *119*, 5706–5714.

Zlotoff, D.A., Sambandam, A., Logan, T.D., Bell, J.J., Schwarz, B.A., and Bhandoola, A. (2010). CCR7 and CCR9 together recruit hematopoietic progenitors to the adult thymus. Blood *115*, 1897–1905.

Figure Legends

Figure 1. Embryonic ETPs retain multi-ILC lineage potential *in vitro*

(a) Experimental strategy for combined lineage potentials of embryonic ETPs. Single ETPs from either E13 or E18 were sorted into OP9 stromal cell. After 36 hours, clones were subdivided in conditions that sustain differentiation of T cells (OP9-DL4) or ILC (OP9).

(b) Representative Flow cytometry plots outlining the strategy used to identify ILC1, ILC2, ILC3 and NK cells of E18 ETPs single cell-derived multi-ILC lineage clone.

(c) Pie chart indicating all phenotypic combinations in individual clones detected after *in vitro* differentiation of E13 and E18 ETPs. Data summarized from at least two independent experiments.

Figure 2. ILC lineage priming in Embryonic ETPs

Single-cell multiplex qPCR analyzed by hierarchical clustering of single E13 and E18 ETPs (80 cells each). Expression of ILC lineage specific transcripts (right margin) in differentiating ETPs. Each column represents a single cell (far right, sorted cell type), and each row represents one gene (of 41 genes; right, expression). Data are from two independent experiments from pooled E13 or E18 thymic lobes. Analysis was done in R package Phenograph as in (Perchet et al., 2018)

Figure 3. Embryonic ETPs give rise to all ILC subsets *in vivo*

(a) Schematic diagram of *in vivo* transfer experiment. P1 Rag2$^{-/-}$γc$^{-/-}$ mice were sub-lethally irradiated, injected with sorted E13 or E18 ETPs and analyzed 5 weeks later.

(b) Flow cytometry analysis of live CD45.2^{+} splenic cells for lymphoid and myeloid markers.

(c) Numbers of the different ILC subsets in tissues (gut, liver, spleen and lung) of reconstituted Rag2$^{-/-}$γc$^{-/-}$ mice.

(d) Representative flow cytometry plots showing ILC analysis in the gut and the liver within viable CD45.2^{+} CD19^{-} Ly6G/C^{-} CD3^{-} cells using the indicated surface markers and intracellular transcription factors. Data from at least 5 mice in each group from two independent experiments.

Figure 4. Neonatal thymectomy has no effect on embryonic derived Vγ5 and Vγ6 γδ T cells

(a) Schematic diagram of neonatal thymectomy experiment. P2 newborn mice were thymectomized and analyzed 6 weeks later.

(b) Frequencies of double positive CD4/CD8 T cells found in the thymus and peri thymic tissue isolated from sham and thymectomized mice, respectively.

(c) Number of Vγ5 γδ T cells in the epidermis isolated from one ear of sham and thymectomized mice.

(d) Number of Vγ6 IL17 γδ T cells, Vγ4 IL17 γδ T cells and αβ T cells in one inguinal lymph node, isolated from sham and thymectomized mice.

(e) Number of αβ CD4^{+} CD44^{-} T cells in the spleen. *P < 0.05, **P < 0.01 and ***P < 0.001 (Student's *t*-test). Data are representative of at least 4 mice in each group from two independent experiments. Data are depicted as mean ± s.e.m.

Figure 5. Emergence of *Il7Rα*$^{+}$ expressing YS-progenitors in E9.5 embryos

(a) Schematic representation of the anatomical sites analyzed in mouse embryos: YS, head, fetal liver and the AGM region.
(b) Representative flow cytometry plot showing YFP expression on live Lin$^-$ CD117$^+$ CD41$^+$ E9.5 YS cells from *Il7r*^{cre}ROSA26^{LSLYFP}.
(c) Number and Percentage of YFP$^+$ per YS (mean ± s.e.m). Data representative of 14 embryos from 4 independent experiments.
(d) Representative flow cytometry plot showing YFP expression on live Lin$^-$ CD117$^+$ E9.5 placenta and AGM region cells.
(e) Expression of CD115, CD127, CD135, CD16/32 and CD31 within the E9.5 YS Lin$^-$ CD117$^+$ CD41$^+$ YFP$^+$ and YFP$^-$ populations.
(f) Experimental strategy for single cell lineage potential assay of E9.5 YS Lin$^-$ CD117$^+$ CD41$^+$ YFP$^+$ and YFP$^-$ populations.
(g) Frequency of wells containing B cells or T cells (h) in cultures of single sorted E9.5 YS Lin$^-$ CD117$^+$ CD41$^+$ YFP$^+$ and YFP$^-$ cells (180 cells from each population analyzed in three independent experiments).
(i) Frequency of erythroid and megakaryocytic (E/Mk), myeloid (GM) or mixed E/Mk/GM colonies of single sorted E9.5 YS Lin$^-$ CD117$^+$ CD41$^+$ YFP$^+$ and YFP$^-$ cells.
(j) Frequency of thymic lobes irradiated and reconstituted with CD117$^+$ E9.5 YS YFP$^+$ or YFP$^-$, or with E12.5 LSK or E10.5 YS as controls, that contained CD4/CD8 DP cells (left plot) or TCR-Vγ5$^+$ T cells (right plot). FTOCs were analyzed at day 12 after reconstitution.

Figure 6. Thymopoiesis-initiating cells develop exclusively from HSC-derived progenitors
(a) Experimental design of lineage tracing analysis of *Csf1r*-expressing cells after OH tamoxifen (OH-TAM) administration at E8.5, or E9.5, or E10.5. Arrows indicate pulse and analysis time points.
(b) Flow cytometry analysis of E12.5 early thymic progenitors (ETPs). E12.5 thymic lobes of embryos pulsed at indicated time points were analyzed. Left plots show the gating strategy to identify ETP. Right representative histograms showing the frequency of Tomato$^+$ or YFP$^+$ cells in ETP. For each experiment one representative analysis is shown.
(c) Frequencies of YFP or Tomato labelled hematopoietic progenitors and Lymphoid tissue inducer (LTi) in E12.5 fetal liver, FB and thymi (left plots) and of LSK, B1 B cells, B cells and Vγ5$^+$ T cells in adult tissues (right plots) of animals pulsed at E8.5, E9.5 or E10.5. Microglia served as controls for labelling efficiency.
All data are pooled from minimally two independent experiments, for embryos analyzed at E12.5 (pulsed at E8.5, n = 8; E9.5, n = 10; E10.5, n = 10) and for adult tissues animals were analyzed between 10-12 weeks of age (pulsed at E8.5, n = 6; E9.5, n = 6; E10.5, n = 2). Data are depicted as mean ± s.e.m except for adult animals pulsed at E10.5 (mean). Abbreviations: ETPs, early thymic progenitors; PerC, peritoneal cavity; BM, bone marrow; FB, fetal blood; FL, fetal liver; FT, fetal thymus.

Figure 7. Model depicting the origin and the lineage potential of thymopoiesis-initiating progenitors.
Abbreviations: TSPs, thymic settling progenitors; ILE, innate lymphoid effectors.

Figure 1

a

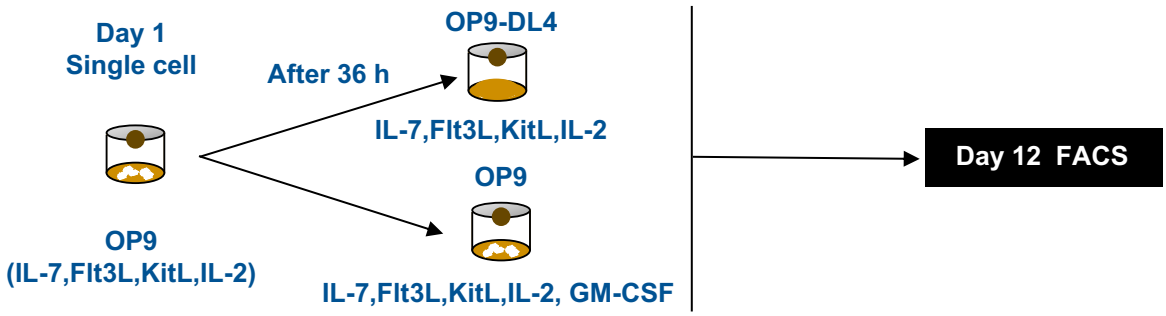
Day 1
Single cell
After 36 h
OP9-DL4
IL-7,Flt3L,KitL,IL-2
OP9
OP9
(IL-7,Flt3L,KitL,IL-2)
IL-7,Flt3L,KitL,IL-2, GM-CSF
Day 12 FACS

b

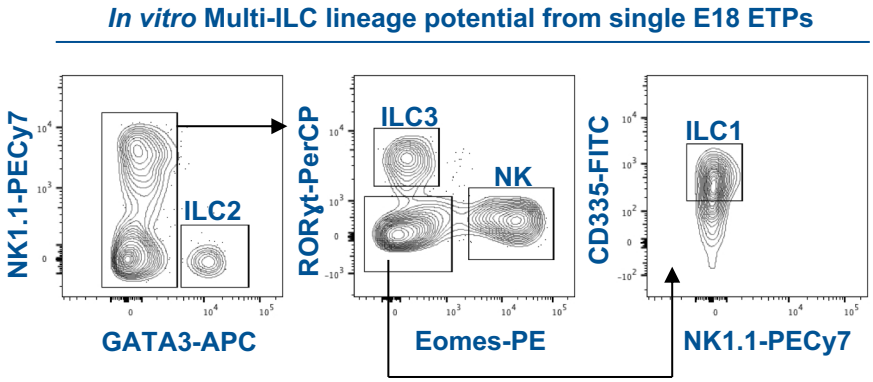
In vitro Multi-ILC lineage potential from single E18 ETPs
NK1.1-PECy7
ILC2
GATA3-APC
RORγt-PerCP
ILC3
NK
Eomes-PE
CD335-FITC
ILC1
NK1.1-PECy7

c

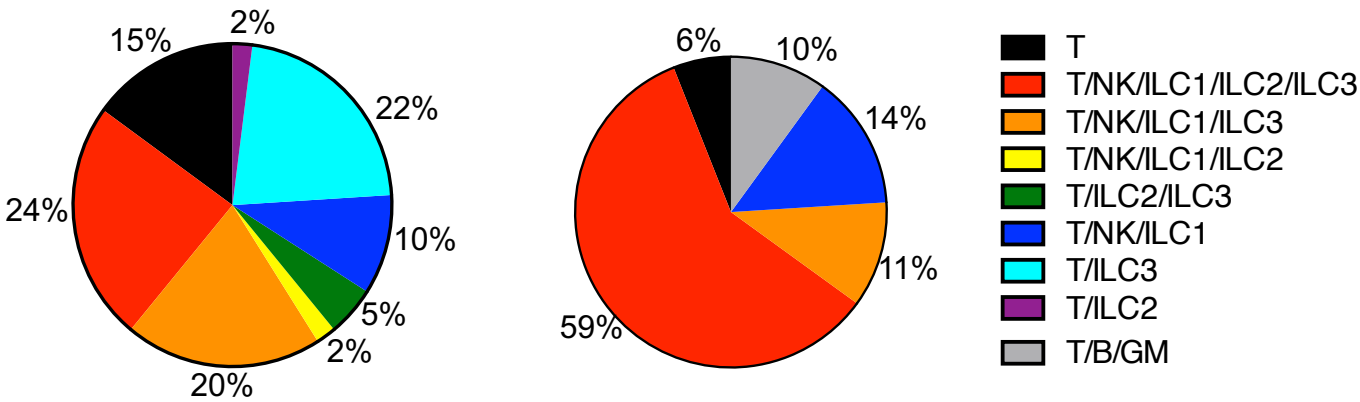
E13 ETPS
81 clones
15%
2%
22%
24%
10%
5%
2%
20%
E18 ETPs
86 clones
6%
10%
14%
11%
59%
T
T/NK/ILC1/ILC2/ILC3
T/NK/ILC1/ILC3
T/NK/ILC1/ILC2
T/ILC2/ILC3
T/NK/ILC1
T/ILC3
T/ILC2
T/B/GM

Figure 2

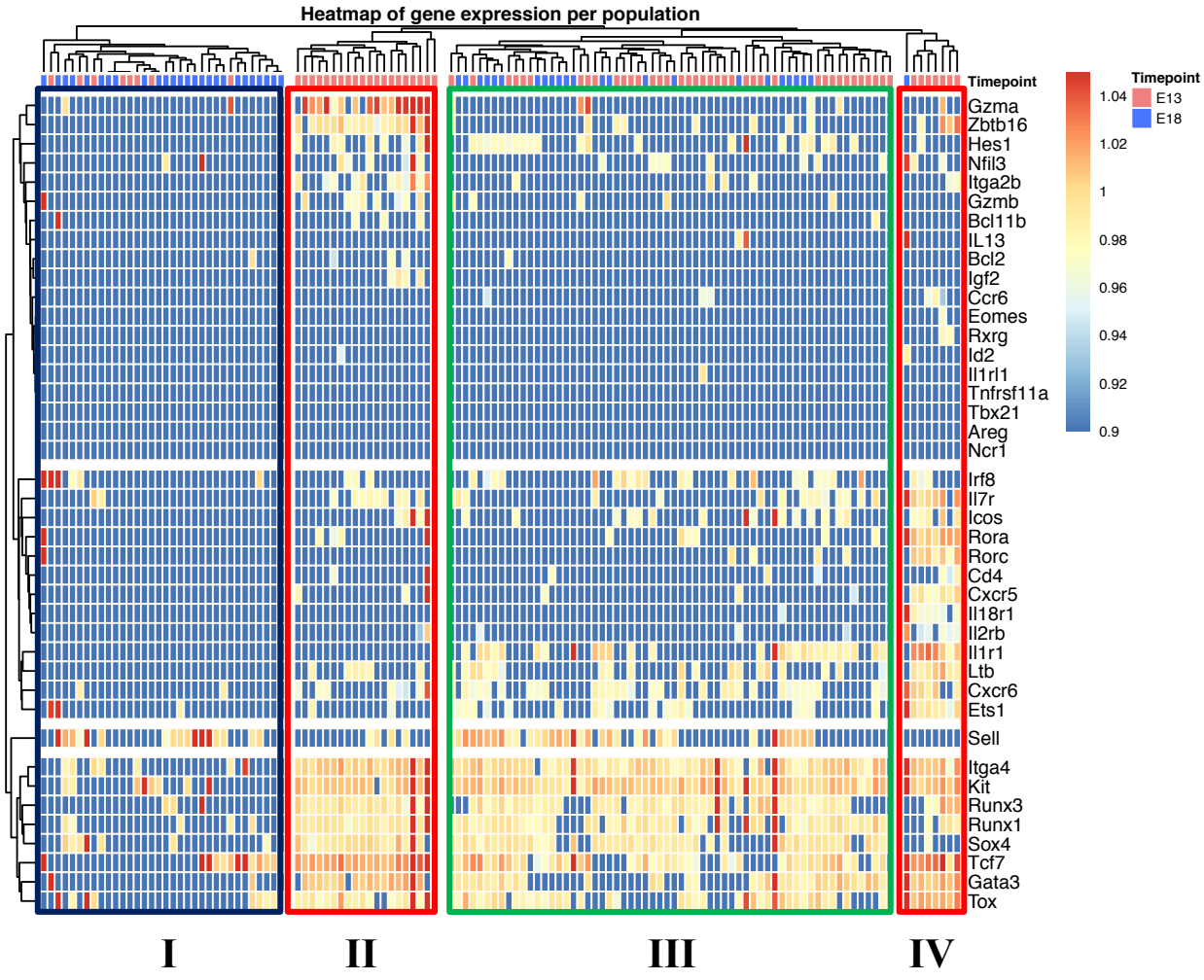
Heatmap of gene expression per population
Timepoint
E13
E18
1.04
1.02
1
0.98
0.96
0.94
0.92
0.9
Gzma
Zbtb16
Hes1
Nfil3
Itga2b
Gzmb
Bcl11b
IL13
Bcl2
Igf2
Ccr6
Eomes
Rxrg
Id2
Il1rl1
Tnfrsf11a
Tbx21
Areg
Ncr1
Irf8
Il7r
Icos
Rora
Rorc
Cd4
Cxcr5
Il18r1
Il2rb
Il1r1
Ltb
Cxcr6
Ets1
Sell
Itga4
Kit
Runx3
Runx1
Sox4
Tcf7
Gata3
Tox
I
II
III
IV

Figure 3

a

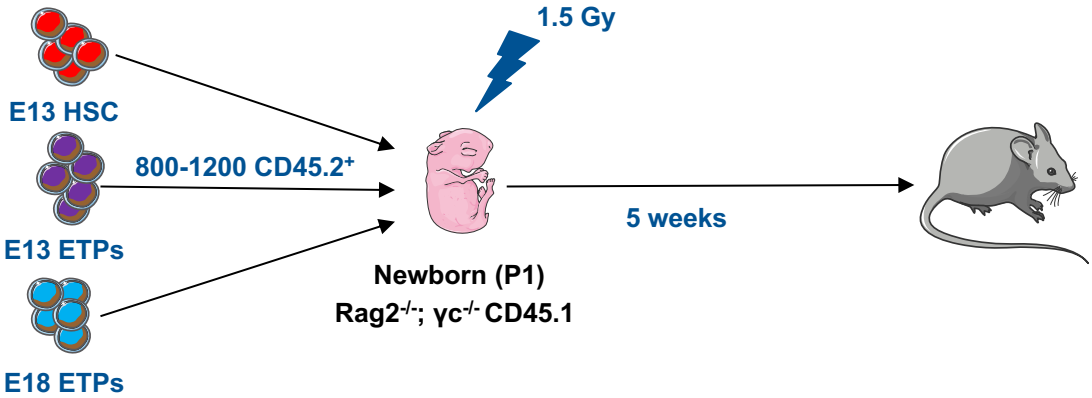

b

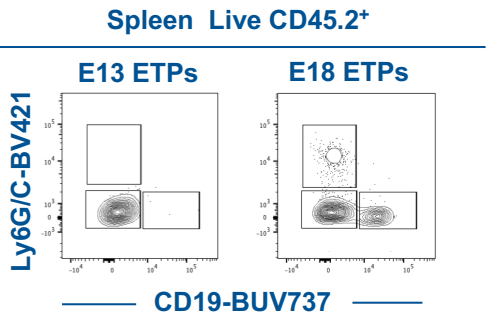

c

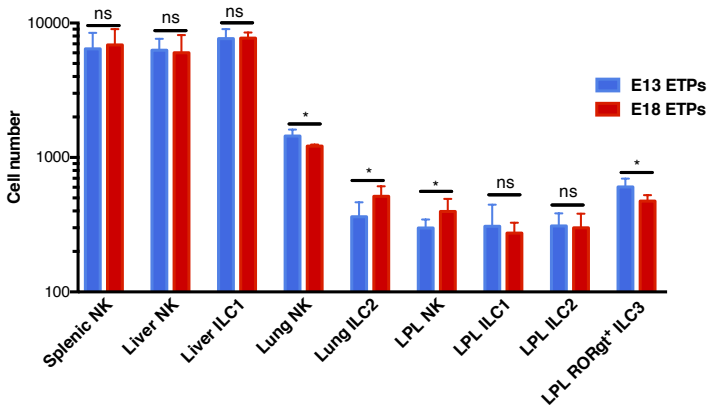

d

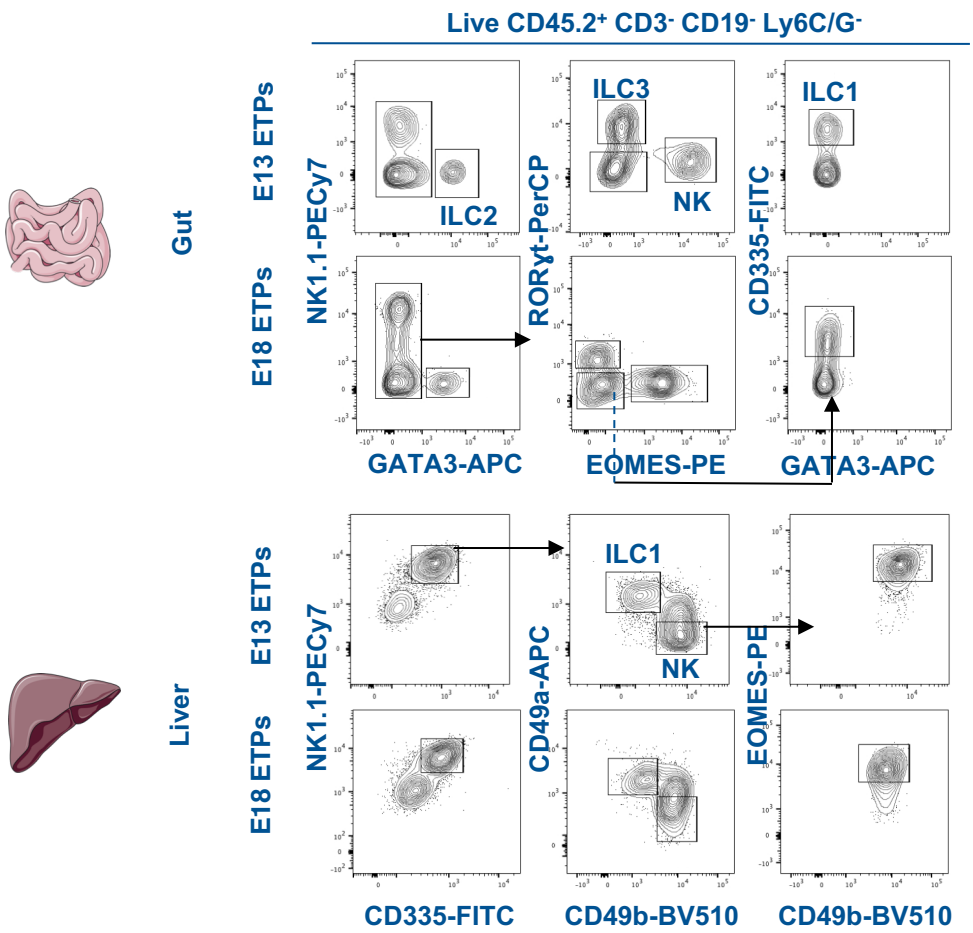

Figure 4

a

b

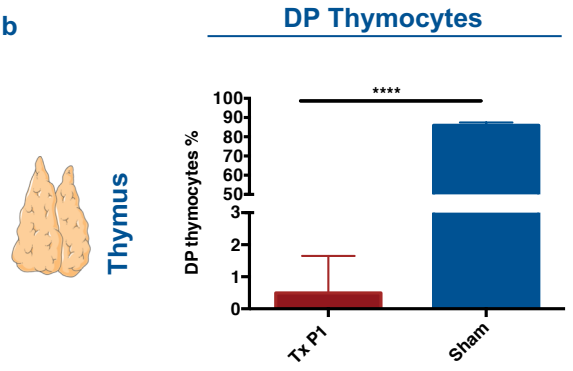

c

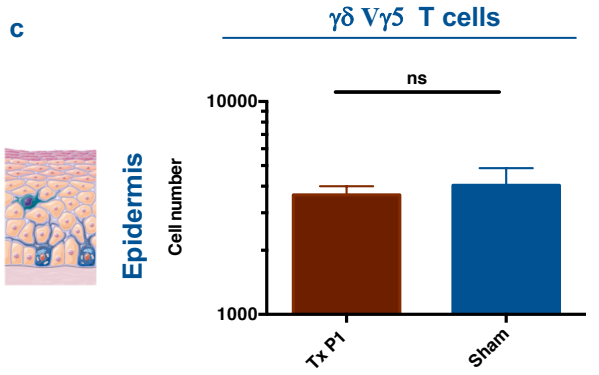

d

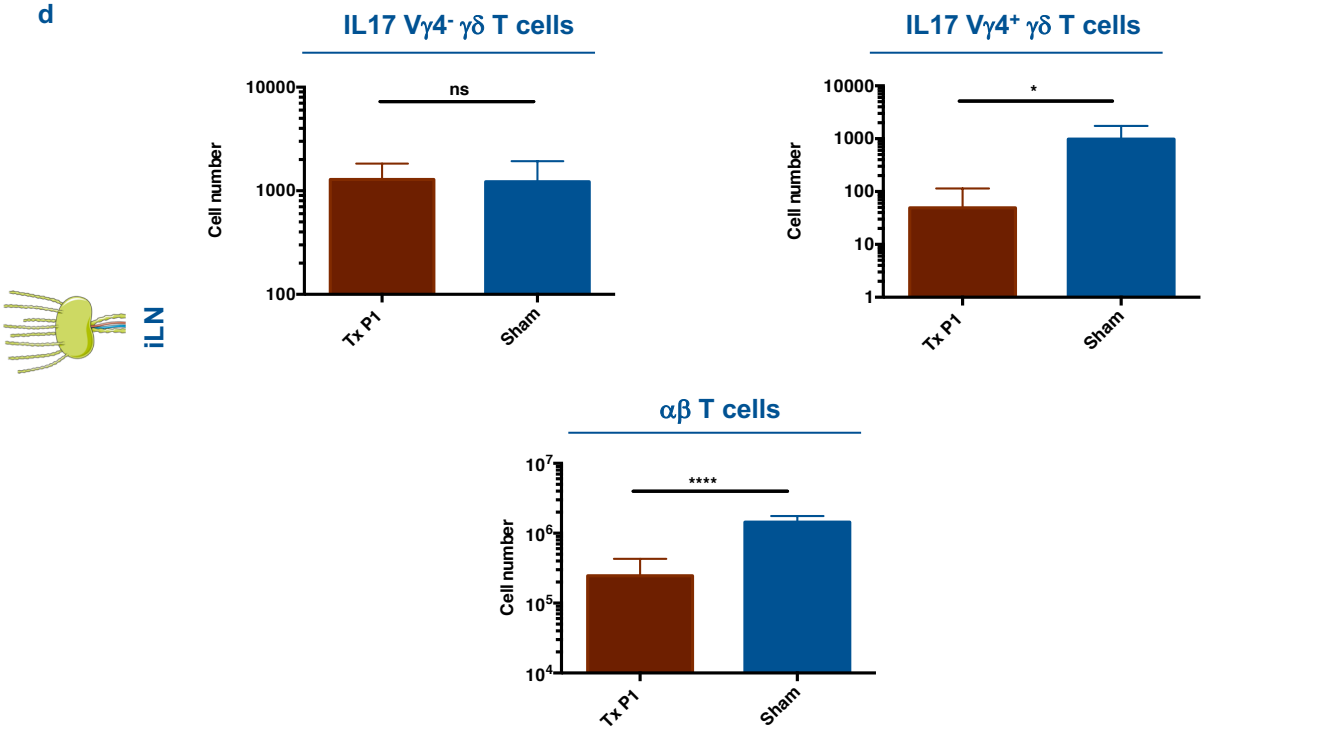

e

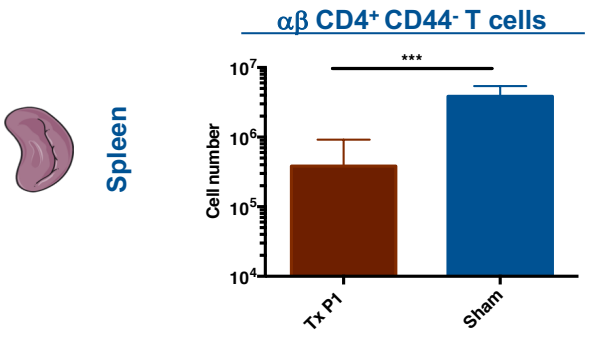

Figure 5

a *Il7r*^{cre}ROSA26^{LSLYFP}

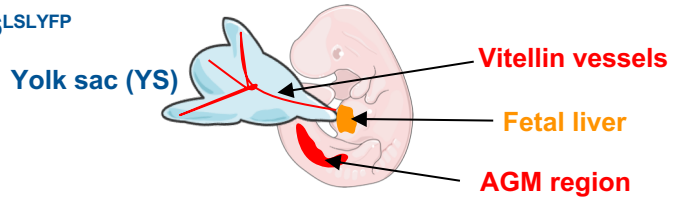

b Lin$^-$ YS E9.5

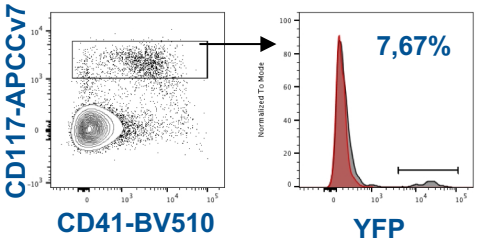

c

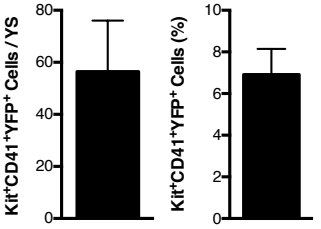

d Lin$^-$ Kit$^+$ E9.5

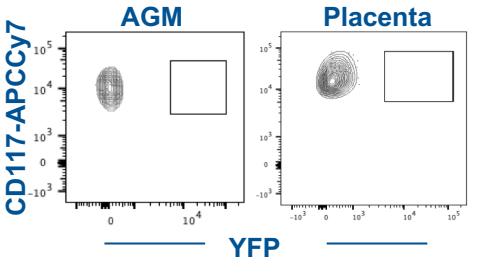

e E9.5 Lin$^-$ Kit$^+$ CD41$^+$

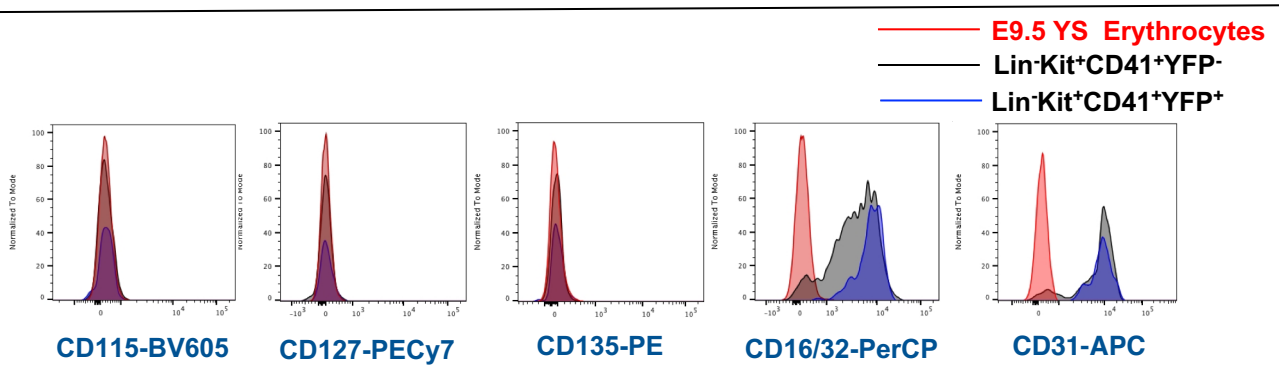

f

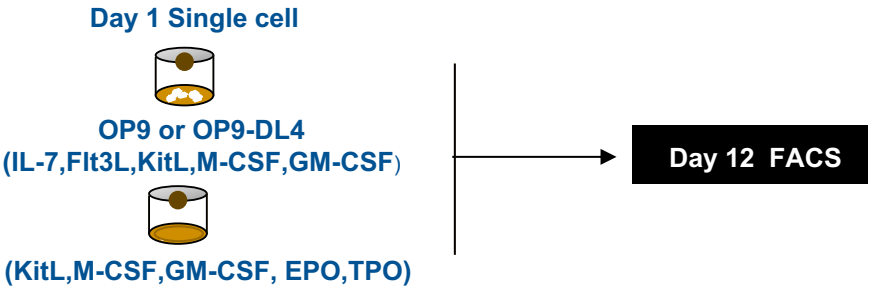

g

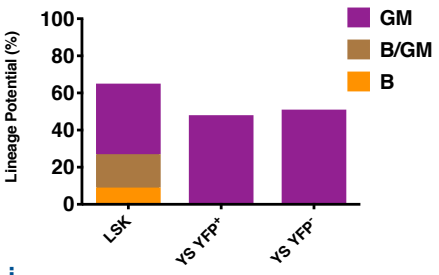

h

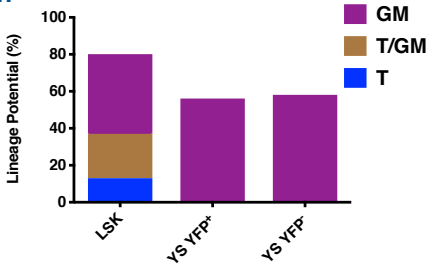

i

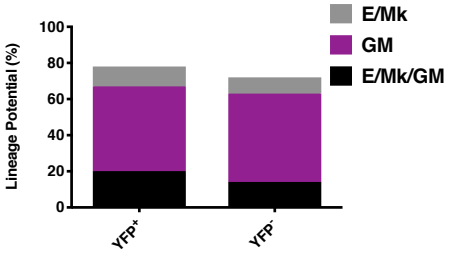

j

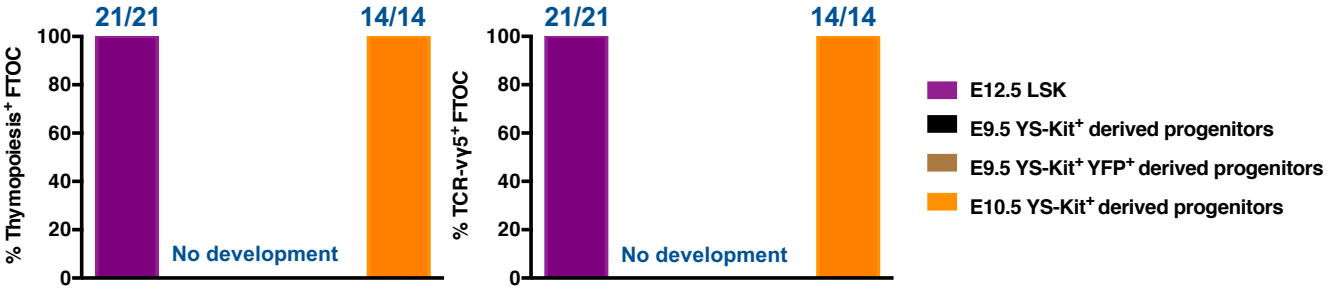

Figure 6

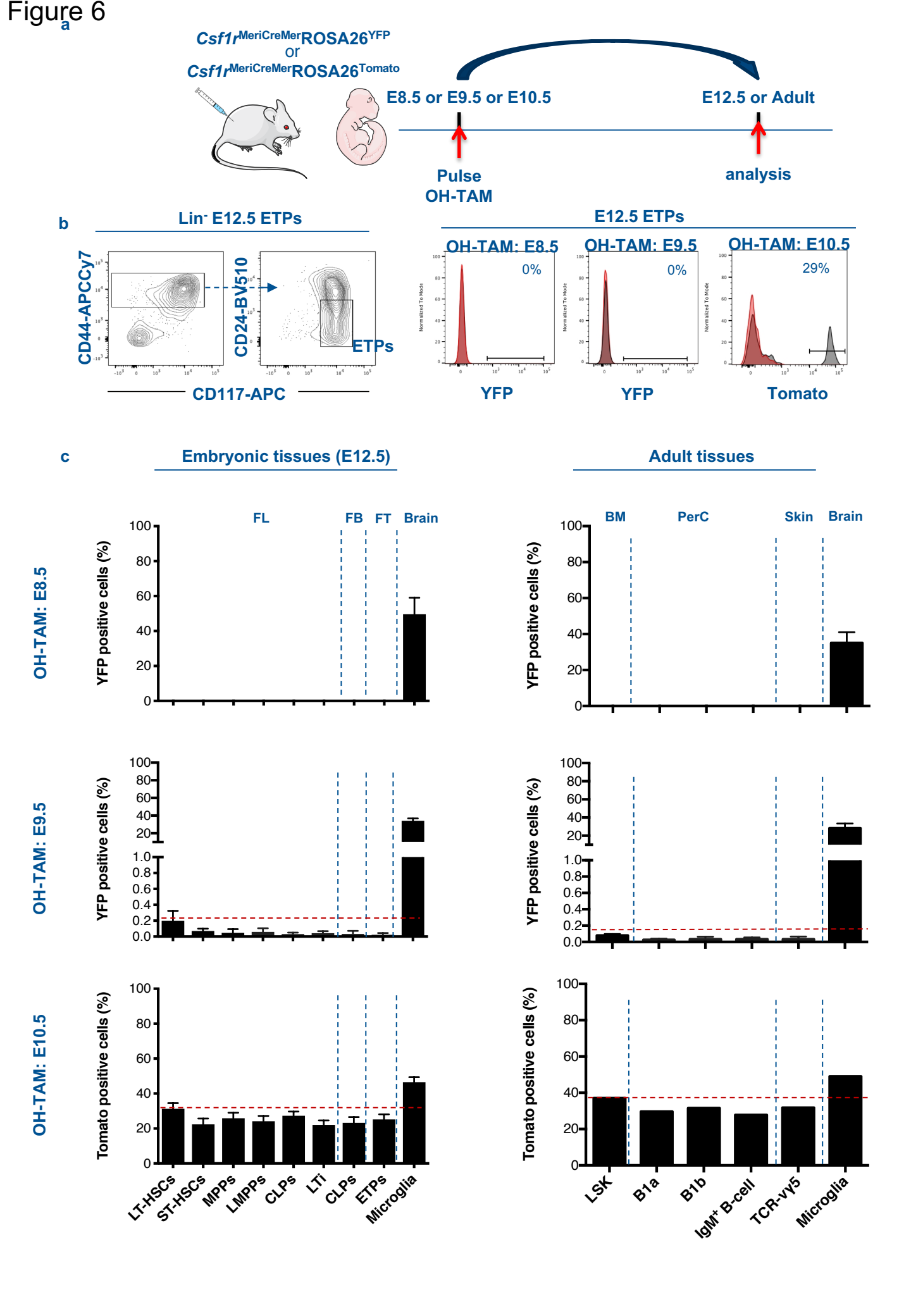
a
Csf1r MeriCreMer ROSA26 YFP
or
Csf1r MeriCreMer ROSA26 Tomato
E8.5 or E9.5 or E10.5
E12.5 or Adult
Pulse
OH-TAM
analysis
b
Lin- E12.5 ETPs
CD44-APCCy7
CD24-BV510
ETPs
CD117-APC
E12.5 ETPs
OH-TAM: E8.5
OH-TAM: E9.5
OH-TAM: E10.5
0%
0%
29%
YFP
YFP
Tomato
c
Embryonic tissues (E12.5)
Adult tissues
FL
FB
FT
Brain
BM
PerC
Skin
Brain
OH-TAM: E8.5
OH-TAM: E9.5
OH-TAM: E10.5
YFP positive cells (%)
Tomato positive cells (%)
LT-HSCs
ST-HSCs
MPPs
LMPPs
CLPs
LTi
CLPs
ETPs
Microglia
LSK
B1a
B1b
IgM+ B-cell
TCR-vγ5
Microglia

Figure 7

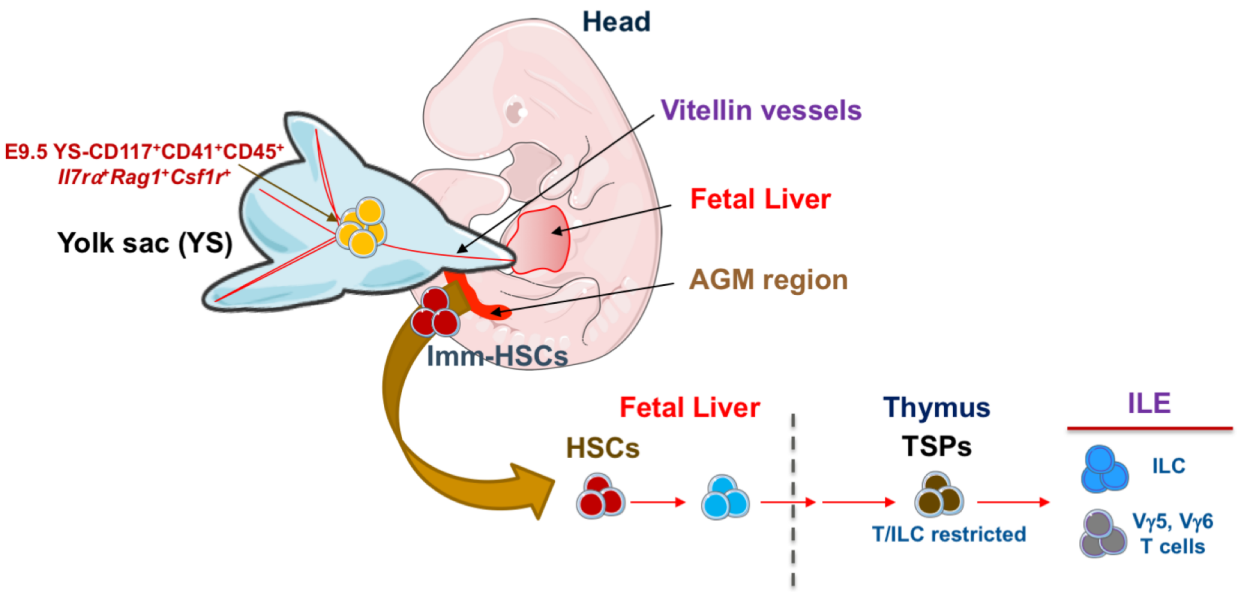
Head
Vitellin vessels
E9.5 YS-CD117+CD41+CD45+
Il7rα+Rag1+Csf1r+
Fetal Liver
Yolk sac (YS)
AGM region
Imm-HSCs
Fetal Liver
HSCs
Thymus
TSPs
T/ILC restricted
ILE
ILC
Vγ5, Vγ6
T cells

Sup Fig 1

a

	E13	E18
Ccl5	3,86	
Ccr5	2,10	
Gzmb	24,62	
Gzma	16,84	
Lta	3,41	
Itga2b	7,75	
Pira1	2,12	
Ikzf4	2,29	
Bhlhe40	3,28	
Zbtb16	3,90	
Cited4	5,48	
B4galnt2	6,54	
Tgm2	7,19	
Txk	8,88	
Gata3	2,14	
Rorc	1,54	
Tcf7	1,70	
Il12rb2	1,52	
Sell		12,11
Ly6a		11,02

b

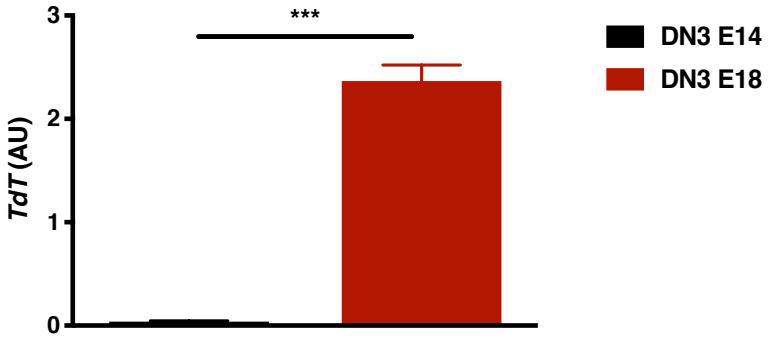

Sup Fig 2

a

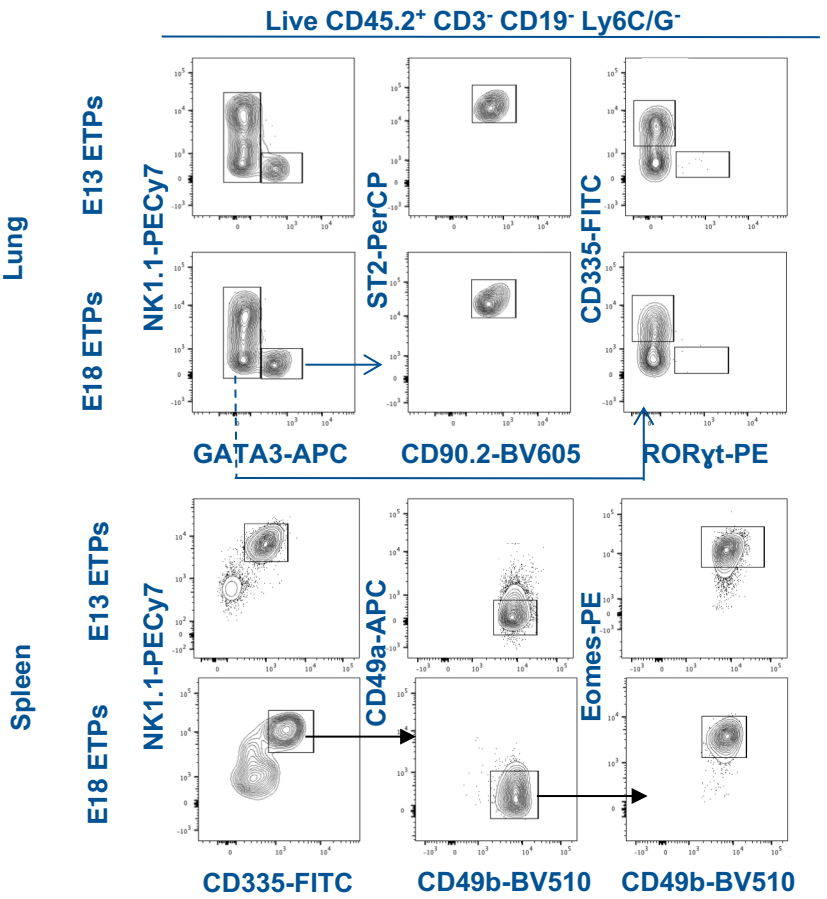
Live CD45.2+ CD3- CD19- Ly6C/G-
Lung
Spleen
E13 ETPs
E18 ETPs
NK1.1-PECy7
ST2-PerCP
CD335-FITC
GATA3-APC
CD90.2-BV605
RORγt-PE
CD49a-APC
Eomes-PE
CD49b-BV510

b

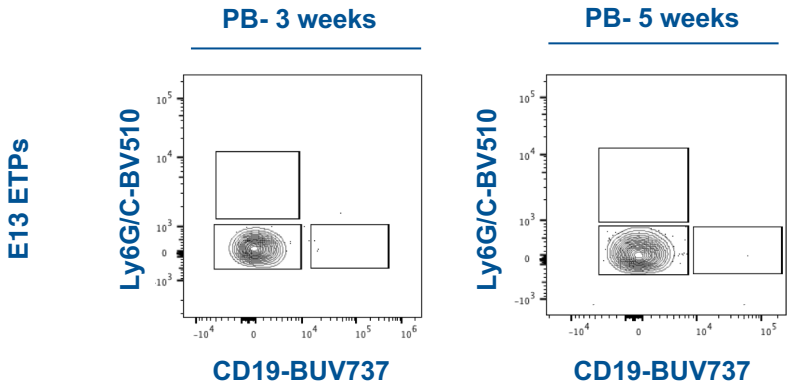
PB- 3 weeks
PB- 5 weeks
E13 ETPs
Ly6G/C-BV510
CD19-BUV737

C

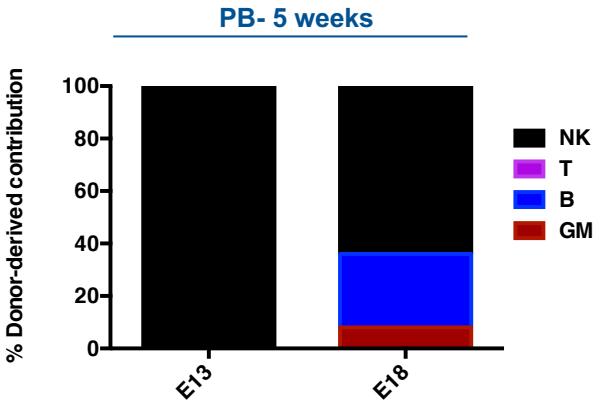
PB- 5 weeks
% Donor-derived contribution
100
80
60
40
20
0
E13
E18
NK
T
B
GM

Sup Fig 3

a

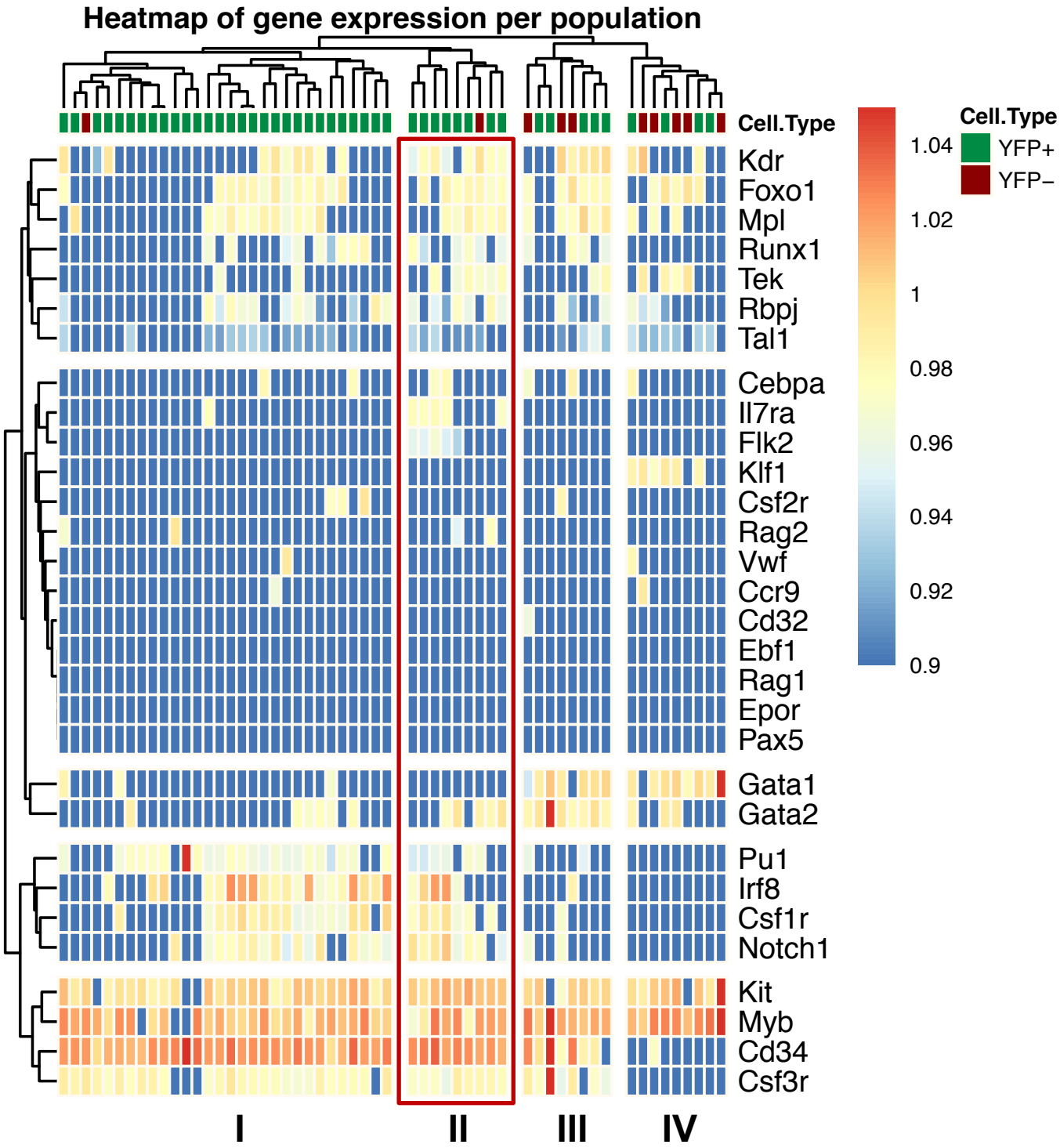

b

	YFP +
Il7r +	6
Il7r -	41

Sup Fig 4

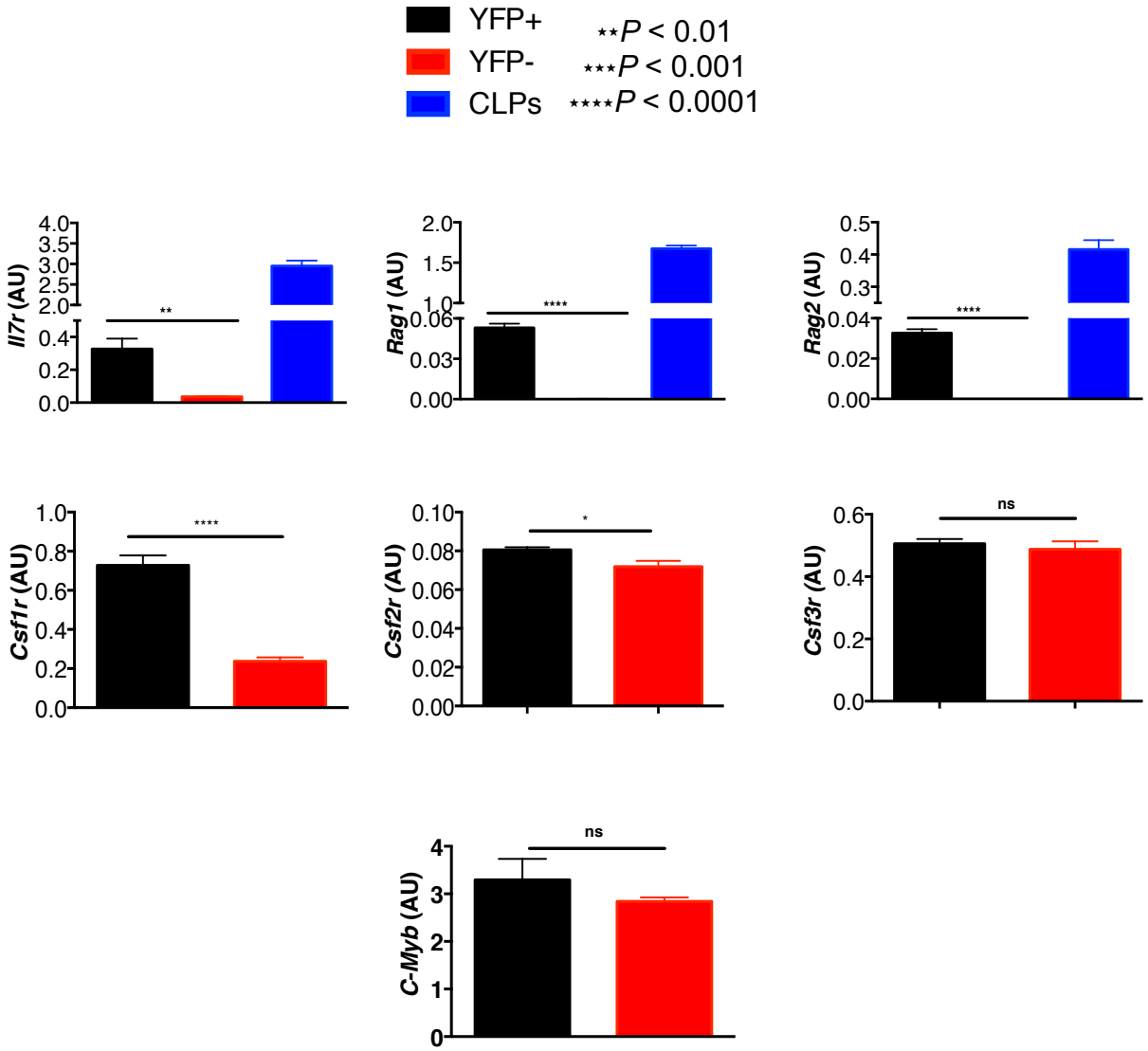
YFP+
YFP-
CLPs
**P < 0.01
***P < 0.001
****P < 0.0001
Il7r (AU)
Rag1 (AU)
Rag2 (AU)
Csf1r (AU)
Csf2r (AU)
Csf3r (AU)
C-Myb (AU)
ns

Sup Fig 5

IL7r^{cre}ROSA26^{LSLYFP}

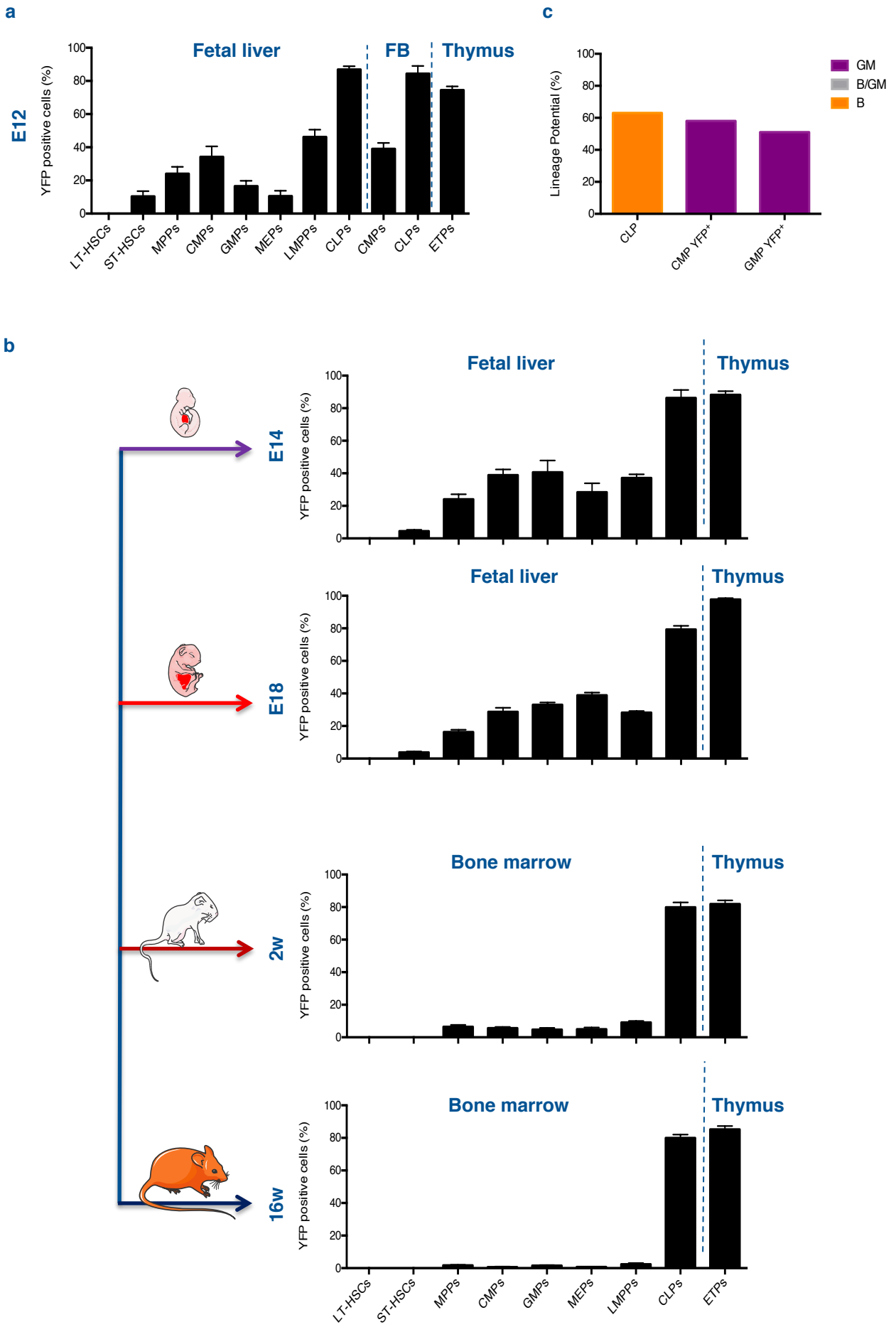

Sup Fig 6

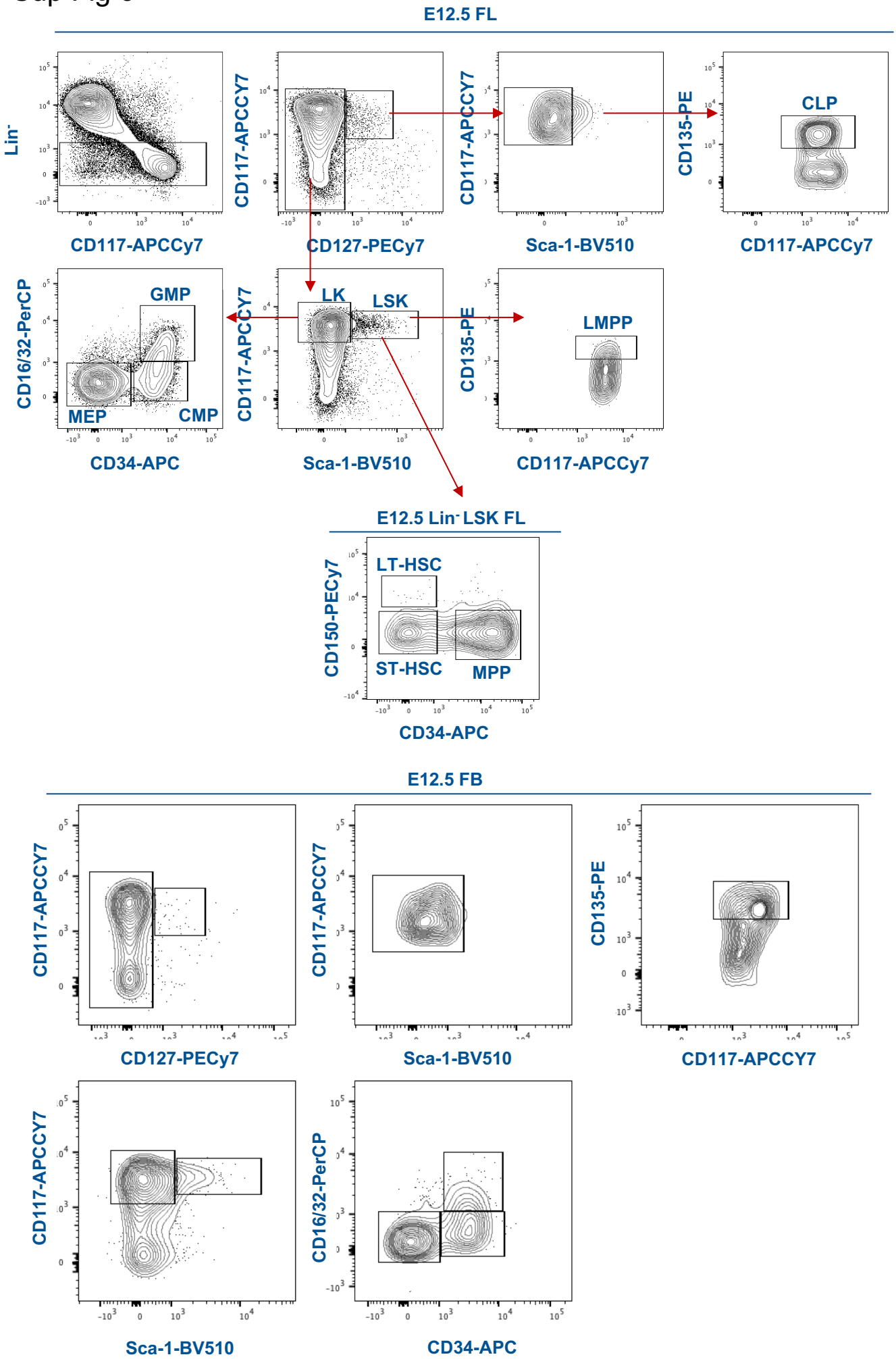
E12.5 FL
Lin-
CD117-APCCy7
CD117-APCCY7
CD127-PECy7
CD117-APCCY7
Sca-1-BV510
CD135-PE
CLP
CD117-APCCy7
CD16/32-PerCP
GMP
MEP
CMP
CD34-APC
CD117-APCCY7
LK
LSK
Sca-1-BV510
CD135-PE
LMPP
CD117-APCCy7
E12.5 Lin- LSK FL
CD150-PECy7
LT-HSC
ST-HSC
MPP
CD34-APC
E12.5 FB
CD117-APCCY7
CD127-PECy7
CD117-APCCY7
Sca-1-BV510
CD135-PE
CD117-APCCY7
CD117-APCCY7
Sca-1-BV510
CD16/32-PerCP
CD34-APC

Sup Fig 7

IL7r^{cre}ROSA26^{LSLYFP}

a

E18

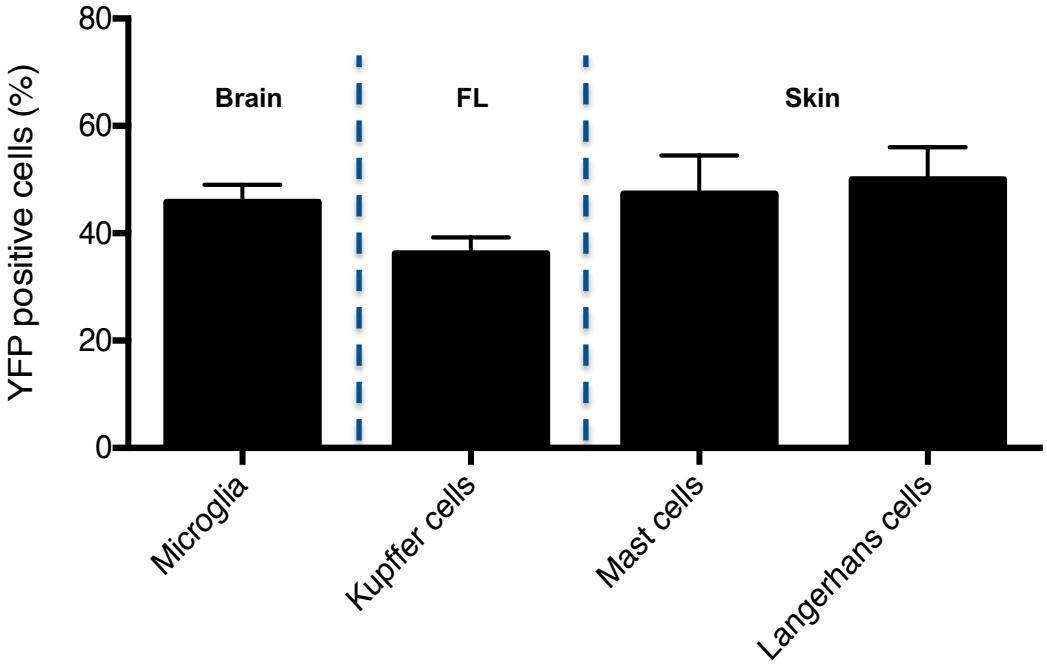

b

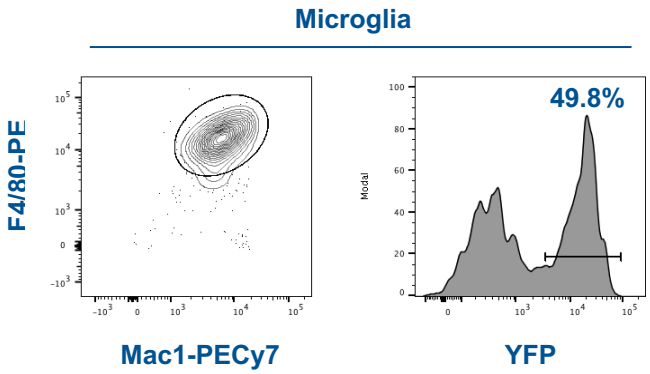

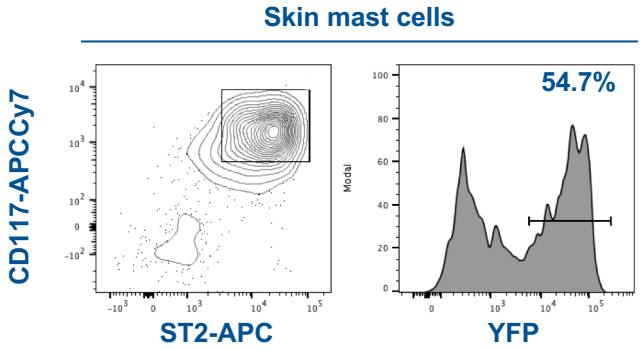

Csf1r^{MeriCreMer}ROSA26^{YFP}

Pulsed E8.5, Analyzed E9.5

a

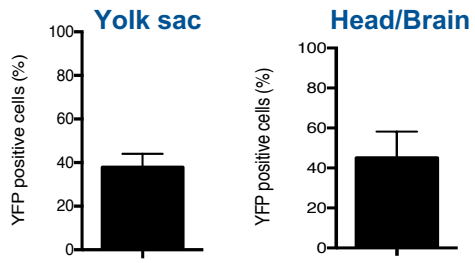

b

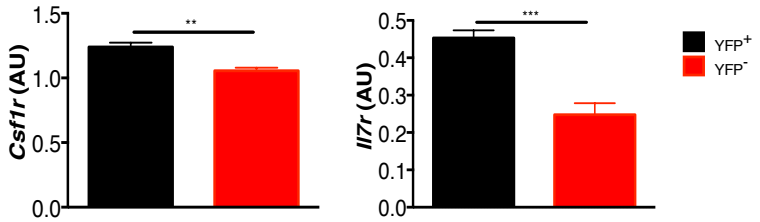

c

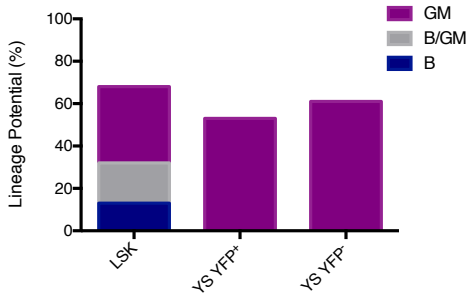

d

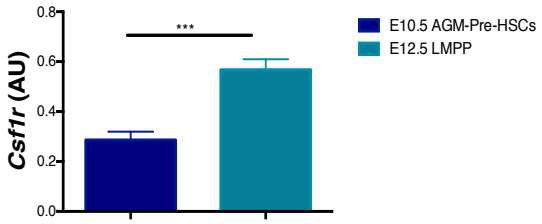

e

Lin$^-$ CD117$^+$ CD127$^+$ CD135$^-$ $\alpha_4\beta_7^+$ FL E12.5 LTi

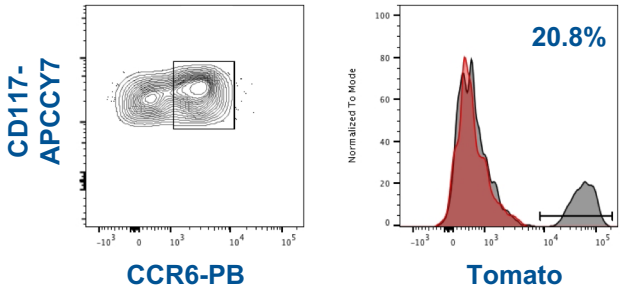

f

PerC: IgM$^+$CD11b$^+$

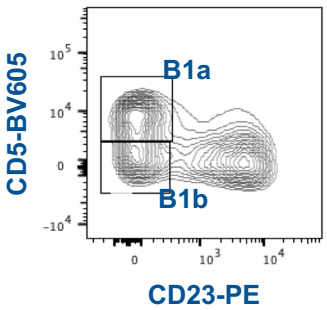

Skin: CD45$^+$CD3$^+$

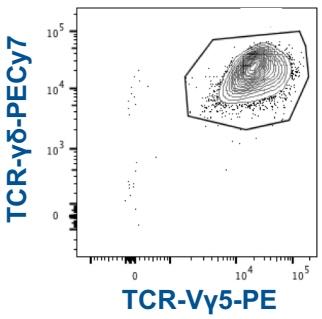

Figure S1. Selected genes (from the database of the Immunological Genome Project) with differential expression in TSPs at E13 versus E18.

(a) Genes with differential expression in TSPs at E13 versus E18 (Fold change). Transcripts analyzed are involved in either T cell development or innate lymphoid effectors development including NKT cells, ILC and γδ T cells.
(b) qRT-PCR analysis of TdT expression in DN3 thymocytes at E14 versus E18.

Figure S2. Gating strategy to identify different subsets of ILC in different tissues, related to Figure 3

(a) Representative flow cytometry plots of ILC analysis in the lung and the spleen of Rag2$^{-/-}$γc$^{-/-}$ mice transplanted with E13 or E18 ETP. Analysis was done on viable CD45.2^{+} CD19^{-} Ly6G/C^{-} CD3^{-} cells using the indicated surface markers and intracellular transcription factors.
(b) Peripheral blood (PB) analysis of myeloid and B cells, 3 and 5 weeks post transplantation of mice recipients of E13 TSPs.
(c) Frequency of donor-derived T, B, NK and myeloid lineages in the PB 5 weeks after transplantation in mice recipients of either E13 or E18 TSPs.

Figure S3. Quantitative gene expression analysis of single E9.5 YS Lin^{-} CD117^{+} CD41^{+} YFP^{+} and YFP^{-} cells, Related to Figure 5.

(a) Hierarchical clustering of single YFP^{+} and YFP^{-} E9.5 Lin^{-} CD117^{+} CD41^{+} cells analyzed for the expression of lymphoid associated (Il7r, Rag1, Rag2, Flt3), myeloid associated (Cebpa, Cd32, Csf1r, Csf2r, Csf3r, Irf8, Pu1), B cell associated (Pax5, Ebf1), E/Mk associated (EpoR, Gata1, Mpl, Tal1, Vwf, Klf1) and hematopoiesis associated (Gata2, Myb, Runx1, Kit, Cd34) genes.
(b) Number of *Il7r*$^{+}$ and *Il7r*$^{-}$ cells within E9.5 YS YFP expressing cells.

Figure S4. qRT-PCR analysis of lymphoid, myeloid and erythro-megakaryocytic-lineage associated genes in E9.5 YS Lin^{-} CD117^{+} CD41^{+} YFP^{+} and YFP^{-} populations, Related to Figure 5.

YFP^{+} and YFP^{-} E9.5 YS Lin^{-} CD117^{+} CD41^{+} cells were sorted and subjected to RT-PCR analysis (100 cells per reaction). Histograms show the expression of designated transcripts normalized for the expression of HPRT. CLP were taken as positive control for the expression of *il7r*, *Rag1* and *Rag2*.

Figure S5. *Il7Rα*$^{+}$ expression in fetal liver multipotent and myeloid progenitors, Related to Figure 5.

(a) Frequencies of YFP labelled E12.5 hematopoietic progenitors in the fetal liver, fetal blood (FB) and the thymus of il7r^{Cre}-Rosa^{LSLYFP} embryos.
(b) Frequency of wells containing B cells or GM in cultures of single sorted E12.5 fetal liver CLPs, CMP YFP^{+} and GMP YFP^{+} on OP9 cells and analyzed after 12 days of culture (three independent experiments).
(c) Frequencies of YFP labelled hematopoietic progenitors analyzed in the fetal liver and fetal thymus of E14.5 and E18.5 embryos or in the bone marrow and thymus of 2 and 16-week old mice. Data are pooled from at least two independent experiments (mean ± s.e.m).

Figure S6. Gating strategy for hematopoietic progenitors, Related to Figure S5.

Figure S7. YFP expression in brain, skin and liver resident macrophages and in skin resident mast cells from E18 *Il7r*^{cre}ROSA^{LSLYFP} embryos. Related to Figure S5.

(a) Frequency of YFP expressing Microglia, liver macrophages, skin macrophages and mast cells of E18 embryos. Data pooled from three independent experiments, data are depicted as mean ± s.e.m.

(b) Gating strategy used for the identification of microglia and skin mast cells.

Figure S8. Lineage tracing analysis of *Csf1r*-expressing YS-progenitors. Related to Figure 6.

(a) Frequency of YFP+ cells in YS (left histogram) and in the head/Brain (right histogram) of *Csf1r*^{MerCreMer}ROSA26^{YFP} E9.5 embryos, pulsed at E8.5.

(b) qRT-PCR analysis of *Csf1r* (left graph) and *Il7ra* (right graph) transcripts in E9.5 YS Lin^{-} CD117^{+} CD41^{+} YFP^{+} and YFP^{-} populations.

(c) Frequency of B, GM and multiple B/GM cells obtained from single sorted E9.5 YS Lin^{-} CD117^{+} CD41^{+} YFP^{+} and YFP^{-} cells on OP9 stromal cells, cultured with the appropriated cytokines.

(d) qRT-PCR analysis of *Csf1r* transcripts in E10.5 AGM-Pre-HSCs (sorted as CD31^{+}CD117^{+}CD41^{+}CD45^{low}) and E12.5 FL LMPPs.

(e) Flow cytometry gating strategy to identify E12.5 FL lymphoid tissue inducer cells (LTi)(left panel) and frequency of tomato^{+} cells within LTi (right panel).

(f) Flow cytometry gating strategy to identify B1 B cells in the peritoneal cavity and Vγ5^{+} T cells in the skin.

Table 1. Antibody and reagents list

Mouse antibody	*Clone*	*Supplier*	*Identifier Cat#*
Anti-CD45	30-F11	BD Biosciences	103116
Anti-CD44	IM7	BD Biosciences	553133
Anti-CCR6	29-2L17	SONY	1249070
Anti-CD117	ACK2	SONY	1275610
Anti-CD11b	M1/70	BD Biosciences	557960
Anti-CD41	MWReg30	BD Biosciences	561850
Anti-CD127	A7R34	SONY	175070
Anti-CD135	A2F10	SONY	1276530
Anti-CD150	TC15-12F12.2	Biolegend	115941
Anti-CD16/32	93	SONY	1106620
Anti-CD19	6D5	SONY	1177560
Anti-CD115	AFS98	eBioscience	12-1152-83
Anti-CD23	B3B4	Biolegend	101607
Anti-CD24	M1-69	SONY	1109155
Anti-CD25	PC61	Biolegend	102024
Anti-Vγ5	536	BD Biosciences	553229
Anti-CD3ε	145-2C11	SONY	1101640
Anti-CD34	RAM34	eBioscience	50-03482
Anti-$\alpha_4\beta_7$	DATK32	BD Biosciences	740892
Anti-CD4	RM4-5	BD Biosciences	563727
Anti-TCRγδ	GL3	Biolegend	118123
Anti-F4/80	BM8	eBioscience	25-4801-82
Anti-GATA3	TWAJ	Invitrogen	50-9966-42
Anti-EOMES	Dan11mag	Invitrogen	12-4875-82
Anti-CD45.1	A20	eBioscience	17-0453-82
Anti-CD45.2	104	BD Bioscience	558702
Anti-CD48	HM48-1	eBioscience	17-0481-82
Anti-CD49a	Ha31/8	BD Biosciences	562113
Anti-CD5	53-7.3	BD Biosciences	563194
Anti-CD62L	MEL-14	BD Biosciences	553152
Anti-CD49b	HMa2	BD Biosciences	740133
Anti-CD8	YTS156.7.7	SONY	1233030
Anti-CD335	29A1.4	BD Biosciences	562850
Anti-NK1.1	PK136	SONY	1143680
Anti-Ter119	TER-119	SONY	1181020
Anti-Sca-1	D7	SONY	1140645
Anti-RORγt	Q31-378	BD Biosciences	562683
Anti-Gr1	RB6-8C5	BD Biosciences	563040
Anti-IgM	II/41	BD Biosciences	550676
Anti-T1/ST2	RMST2-2	eBioscience	17-9335-82
Anti-CD90	53-2.1	SONY	1301585

Reagents	*Source*	*Identifier Cat#*
Propidium iodide	Sigma	019k1149
Fixable viability dye	Invitrogen	L34961
Percoll	GE Healthcare	17-0891-01
Penicillin-Streptomycin (5,000 U/ml)	GIBCO	15070-063
2-Mercaptoethanol	GIBCO	31350-010
Opti-MEM reduced serum medium, GlutaMAX supplement	GIBCO	51985-026
Cytokines (IL-7, IL-2, SCF, M-CSF and GM-CSF)	Obtained from the supernatant of myeloma cell lines (provided by F.Melchers) transfected with cDNA encoding those cytokines.	N/A
rmEPO	R&D	959-ME
rmTPO	R&D	488-TO
rmFlt3L	R&D	427-FL
4-OH Tamoxifen	Sigma	176-50mg
Progesterone	Sigma	P0130
Collagenase VIII	Sigma	C2139-1G
Collagenase IV	GIBCO	17104-019
Collagenase I	GIBCO	17018-029
DNase I	Roche	11-284-932-001
Dispase II	Invitrogen	17105041
FcR Blocking reagent, mice	BD Biosciences (clone 2.4g2)	553142
Streptavidin	Invitrogen	S11222
Foxp3/transcription factor staining buffer set	Invitrogen	72-5775-40

Table 2. Experimental models

Experimental Models: Cell lines	*Source*	*Identifier*
Mouse: OP9	Institut Pasteur	Cat# CRL-2749
Mouse: OP9-DL4	Institut Pasteur	De La Coste A. et al., 2005

Experimental Models: Mouse strains	*Source*	*Identifier*
Il7r^{Cre}	Prof. HR. Rodewald	Schlenner et al., 2010
Csf1r^{MeriCreMer}	The Jackson Laboratory	Qian et al., 2011 #019098
Rag2$^{-/-}$; γc$^{-/-}$ CD45.1	Institut Pasteur	Colucci et al., 1999
C57BL6/J	Charles River	Stock# 000664
Ly5.1	Institut Pasteur	N/A
ROSA26^{Tomato}	The Jackson Laboratory	[1] Stock# 007914
ROSA26^{YFP}	The Jackson Laboratory	Stock# 006148

Table 3. Biomark primers

Gene	*Ref*	*Gene*	*Ref*
Actb	*Mm00607939_s1*	*Kit*	*Mm00445212_m1*
Hprt	*Mm00446968_m1*	*Runx3*	*Mm00450960_m1*
Gapdh	*Mm03302249_g1*	*Runx1*	*Mm01213405_m1*
Gzma	*Mm01304452_m1*	*Sox4*	*Mm00486320_s1*
Gzmb	*Mm00442837_m1*	*Tcf7*	*Mm01173766_m1*
Zbtb16	*Mm00784709_s1*	*Gata3*	*Mm00484683_m1*
Hes1	*Mm01342805_m1*	*Tox*	*Mm00455231_m1*
Nfil3	*Mm00600292_s1*	*Ccr9*	*Mm02620030_m1*
Itga2b	*Mm00439741_m1*	*Cd32*	*Mm00438875_m1*
Bcl11b	*Mm00480516_m1*	*Cd34*	*Mm00519283_m1*
Il13	*Mm00434204_m1*	*Cebpa*	*Mm00514283_s1*
Bcl2	*Mm_00477631_m1*	*Csf1r*	*Mm00432689_m1*
Igf2	*Mm00439564_m1*	*Csf2r*	*Mm00438331_g1*
Ccr6	*Mm99999114_s1*	*Csf3r*	*Mm00432735_m1*
Eomes	*Mm01351985_m1*	*Ebf1*	*Mm01288946_m1*
Rxrg	*Mm00436411_m1*	*Epor*	*Mm00438760_m1*
Id2	*Mm0011781_m1*	*Flk2*	*Mm01210883_m1*
Il1rl1	*Mm00516117_m1*	*Foxo1*	*Mm00490672_m1*
Tnfrsf11a	*Mm00437132_m1*	*Gata1*	*Mm00484678_m1*
Tbx21	*Mm00493445_m1*	*Gata2*	*Mm00492301_m1*
Areg	*Mm00437583_m1*	*Kdr*	*Mm01222421_m1*
Ncr1	*Mm01337324_g1*	*Klf1*	*Mm00516096_m1*
Irf8	*Mm00492567_m1*	*Mpl*	*Mm00440310_m1*
Il7r	*Mm00434295_m1*	*Myb*	*Mm00501741_m1*
Icos	*Mm00497600_m1*	*Notch1*	*Mm_00435249_m1*
Rora	*Mm01173766_m1*	*Pax5*	*Mm00435497_m1*
Rorc	*Mm01261022_m1*	*Pu.1*	*Mm03048233_m1*
Cd4	*Mm00442754_m1*	*Rag1*	*Mm01270936_m1*
Cxcr5	*Mm00432086_m1*	*Rag2*	*Mm00501300_m1*
Il18r1	*Mm00515178_m1*	*Rbpj*	*Mm01217627_g1*
Il2rb	*Mm01195267_m1*	*Tal1*	*Mm01187033_m1*
Il1r1	*Mm00434237_m1*	*Tek*	*Mm00443243_m1*
Ltb	*Mm00434774_g1*	*Vwf*	*Mm00550376_m1*
Cxcr6	*Mm02620517_s1*		
Ets1	*Mm01175819_m1*		
Sell	*Mm00441291_m1*		
Itga4	*Mm00439770_m1*		

Methods

Animals. Mice were bred in dedicated facilities of the Institut Pasteur under specific pathogen-free conditions. Mattings were done overnight; on the following day, mice showing a vaginal plug were isolated and were considered to be embryonic day 0 (E0). *Il7r*^{Cre} (Schlenner et al., 2010) ,Rag2$^{-/-}$; γc$^{-/-}$ CD45.1 (Colucci et al., 1999) , *ROSA26*^{Tomato} (Madisen et al., 2010) and *ROSA26*^{YFP} mice were on C57BL/6 background, *Csf1r*^{MeriCreMer} (Qian et al., 2011) mice were on FVB background. All animal manipulations were performed according to the ethic charter approved by French Agriculture ministry and to the European Parliament Directive 2010/63/EU.

Fate-mapping of *Il7r*$^{+}$ hematopoietic progenitors. For fate-mapping analysis of *Il7r+* progenitors, *Il7r*^{Cre} females were crossed to homozygous *ROSA26*^{YFP}. Indicated embryonic tissues and adult tissues were analyzed by flow cytometry.

In utero pulse labelling of *Csf1r+* Progenitors. For fate-mapping analysis of *Csf1r+* progenitors, we crossed *Csf1r*^{MeriCreMer} with either *ROSA26*^{YFP} or *ROSA26*^{Tomato} reporter mice. For induction of reporter recombination in the offspring, a single dose of 75 µg per g (body weight) of 4-Hydroxytamoxifen (Sigma) (4OHT) supplemented with 37.5 µg per g (body weight) progesterone (Sigma) (to counteract the mixed estrogen agonist effects of 4OHT, which can result in fetal abortions) was injected either at E8.5 or E9.5 (Gomez Perdiguero et al., 2015). To induce recombination in the embryos at E10.5, females received a single dose of 1.2 mg 4OHT and 0.6 mg progesterone.

Cell suspension. Cell suspensions from embryonic, newborn and adult tissues were obtained through mechanical dissociation and/or enzymatic digestion. In brief, all cells were suspended in Hanks' balanced-salt solution (HBSS) supplemented with 1% FCS (GIBCO). Embryonic tissues were micro dissected under a binocular magnifying lens. Organs were rinsed with HBSS plus 1% FCS to remove blood cells contamination. Then, thymus and fetal liver were passed through a 26-gauge needle of a 1-ml syringe and were filtered. Blood from embryos was obtained for 20 to 30 min HBSS supplemented with 1% FCS without calcium and magnesium. Blood cells were resuspended in a 70% (vol/vol), topped by a 40% (vol/vol), solutions of Percoll. After 20 min of centrifugation at 3000 r.p.m, cells were collected at the 40%-70% interface. For embryonic skin samples, harvested back skin was minced with scissors in RPMI medium containing 0.1 mg/ml DNase I (Roche) and 1mg/ml Collagenase I (GIBCO). Digestions were performed for 30-45 min at 37°C under continuous agitation. For embryonic head/brain, tissues were cut into small pieces, incubated in RPMI containing 10% FCS and 0.2 mg/ml Collagenase IV (GIBCO) for 30 min and then passed through a 19G needle to obtain a homogenous cell suspension. Adult thymi and spleen were dissected, and single cell suspension were obtained through a nylon mesh. Bone marrow were collected by flushing bones with HBSS. For adult skin, ears were harvested from 8-10 week-old mice, the dorsal and ventral sheets were separated using forceps and the epidermis was removed by incubation for 45 min at 37°C in 2.4 mg/ml of Dispase II (Invitrogen) and 3% FCS. Then, the epidermis was further digested for 30 min in PBS 0.1 mg/ml DNase I (Roche) and 1mg/ml Collagenase I (GIBCO). Adult brain was processed similar to embryonic brain except for an incubation period of 1 hour and cell suspension was resuspended in a 70% (vol/vol) solution of Percoll topped

by a 40% (vol/vol) solution of Percoll. After 20 min of centrifugation at 3000 r.p.m, cells were collected at the 40%-70% interface.
For reconstituted Rag2$\gamma c^{-/-}$ tissue preparations, animals were exsanguinated, and the lung was minced and incubated for 30 min at 37°C with agitation in RPMI containing 2% FCS, then incubated for 1 hour with RPMI medium containing 0.2 mg/ml Collagenase IV (GIBCO) and 0.1 mg/ml DNase I (Roche). Cells were resuspended in a 70% (vol/vol) solution of Percoll topped by a 40% (vol/vol) solution of Percoll. After 20 min of centrifugation at 3000 r.p.m, cells were collected at the 40%-70% interface. Small intestines were minced into small pieces and digested in RPMI medium containing 0.1 mg/ml DNase I (Roche) and 100 mg/ml Collagenase VIII (Sigma). Cell suspension was resuspended in a 70% (vol/vol) solution of Percoll topped by a 40% (vol/vol) solution of Percoll. After 20 min of centrifugation at 3000 r.p.m, cells were collected at the 40%-70% interface. Livers were teased and cells were resuspended in RPMI with 2% FCS, centrifuged for 7 min, then further purified after 20 min of centrifugation at 3000 r.p.m in 44% Percoll. Peritoneal washouts of adult mice were performed by injecting IP PBS with 2% FCS and collecting the resulting peritoneal fluid.

Flow cytometry and cell sorting. All digested samples were filtered, and single cell suspensions were blocked with anti-CD16/32 (BD Biosciences) and stained with antibodies listed in supplementary table 1 and fixable viability dye (Invitrogen). For transcription factor staining, cells were stained for surface markers for 30 min at 4°C then fixed according to manufacturer's instructions (eBiosciences) and stained with fluorescent antibodies to intracellular proteins. Stained cells were analyzed on a LSR Fortessa flow cytometry or sorted using a FACSAria III (BD Biosciences). Data were analyzed with FlowJo software (Treestar).

Culture. All experiments were done in 96-well plates at 37°C and 5% CO2 and in complete OptiMEM medium supplemented with 10% FCS, penicillin (50 units/ml), streptomycin (50 µg/ml) and β-mercaptoethanol (50 µM) (GIBCO).

a) **Frequency assay.** Single cells were sorted into 96-well plates containing a monolayer of 1000 OP9 (for B cell-ILC and myeloid potential) or OP9-DL4 (for T cell potential) stromal cells in complete medium supplemented with saturating amounts of IL-7, Flt3L, IL-2 and KitL for B, T and ILC differentiation and M-CSF, GM-CSF and KitL for myeloid differentiation. For erythroid, megakaryocytic and myeloid potential, cells were directly sorted into wells of 96-well plate and were supplemented with KitL, erythropoietin for erythrocytes differentiation, thrombopoietin for megakaryocytes differentiation, M-CSF and GM-CSF for myeloid differentiation. Cultures were supplemented with fresh cytokines every 7 d. After 12 days of culture, wells showing colonies were stained for CD19 (B cells), NK1.1 (NK cells) , CD4 (T cells), CD8 (T cells), CD3 (T cells), CD11b (Myeloid cells), Gr-1(Myeloid), CD41 (megakaryocytes) and Ter119 (erythrocytes) or analyze ILC-associated transcription factors after cell fixation, GATA-3 (ILC2), RORgt (ILC3) and Eomes^{-}(ILC1). Frequency scores were assigned based on the frequency of positive wells relative to the total number of plated cells.

b) **Single cell T cell-ILC-B cell-myeloid- potential assay.** Single cells were directly sorted onto a monolayer of OP9 stromal cells in Terasaki plates in medium supplemented with IL-7, IL-2, KitL and Flt3L. After 36h, growing cells were split into OP9 or OP9-DL4

cultures under the same conditions mentioned above, and clones were analyzed after 12 days.

Reconstituted FTOC. Irradiated thymic lobes (30Gy) from CD45.1+ mouse embryos at E14 or E15 were colonized for 48h, on a hanging drop, in Terasaki plates by 200 YS-derived progenitors from CD45.1+ embryos at E9.5, or E10.5 or 200 LSKs from CD45.1+ embryos at E12.5, in culture medium. After colonization, thymic lobes were cultured for 12d on a filter (Millipore) floating on 3ml of complete medium in a 37°C incubator with 5% CO_2. Then, thymi were dissociated and analyzed by flow cytometry.

***In vivo* adoptive transfer.** 800-1200 fetal E13 HSCs, E13 and E18 ETPs from CD45.2+ embryos were sorted using FACSAria III, then injected intravenously into irradiated (1.5G) 1 day old $Rag2^{-/-}$; $\gamma c^{-/-}$ $CD45.1^{+}$ mice. Recipient mice were analyzed 5 weeks post-transfer.

Neonatal Thymectomy. Thymectomy was performed on anesthetized mice within 36 hours of birth. The sternum was split and the bilobed thymus removed by mechanical suction and the skin closed with surgical adhesive. After 6 weeks, the skin, the thymus, the inguinal lymph nodes and the spleen were analyzed. Controls were animals of the same age were sham operated without thymectomy.

Quantitative RT-PCR. mRNA of sorted cells was extracted using the RNeasy Micro Kit (Qiagen), and cDNA was obtained using the PrimeScript RT Kit (Takara). qPCR was performed using TaqMan primers and TaqMan Universal Master Mix (Applied Biosystems) for the following genes: *Il7r*, *Rag1*, *Rag2*, *Csf1r*, *Csf2r*, *Csf3r* and *Myb*. Gene expression was normalized to that of *Hprt* and relative expression was calculated using the $2^{-\Delta Ct}$ method.

Microarray. Microarray data in the GEO database with the accession code GSE50910 published by Ramond et al (Ramond et al., 2013).

Multiplex single-cell qPCR. Single cells were sorted in 96-well PCR plates in 9 µl of RT/pre-amp mix from the CellsDirect One-Step qRT-PCR Kit (Life Technologies) and were kept at -80°C at least overnight. For each subset analyzed, a control-well with 20 cells were sorted. Pre-amplified cDNA (20 cycles) was obtained according to manufacturer's note and was diluted 1:5 in TE buffer, pH 8 (Ambion) for qPCR. Multiplex qPCR was performed using the microfluidics Biomark system on Biomark HD for 40 cycles (Fluidigm). TaqMan probes that were used for RT/pre-amp and qPCR are listed in supplementary table 3. Only single cells for which the three housekeeping genes could be detected before 20 cycles were included in the analysis. Analysis was done in R package Phenograph as in (Perchet et al., 2018)

Statistical analysis. Statistical data show either mean or mean ± s.e.m., and the two tailed unpaired Student's *t*-test was used. Statistic tests were performed using Prism software.

Colucci, F., Soudais, C., Rosmaraki, E., Vanes, L., Tybulewicz, V.L., and Di Santo, J.P. (1999). Dissecting NK cell development using a novel alymphoid mouse model: investigating the role of the c-abl proto-oncogene in murine NK cell differentiation. J. Immunol. Baltim. Md 1950 *162*, 2761–2765.

Madisen, L., Zwingman, T.A., Sunkin, S.M., Oh, S.W., Zariwala, H.A., Gu, H., Ng, L.L., Palmiter, R.D., Hawrylycz, M.J., Jones, A.R., et al. (2010). A robust and high-throughput Cre reporting and characterization system for the whole mouse brain. Nat. Neurosci. *13*, 133–140.

Qian, B.-Z., Li, J., Zhang, H., Kitamura, T., Zhang, J., Campion, L.R., Kaiser, E.A., Snyder, L.A., and Pollard, J.W. (2011). CCL2 recruits inflammatory monocytes to facilitate breast-tumour metastasis. Nature *475*, 222–225.